

Non-linear Fusion in Federated Learning: A Hypernetwork Approach to Federated Domain Generalization

Marc Bartholet¹ Taehyeon Kim² Ami Beuret¹ Se-Yeoung Yun² Joachim Buhmann¹

Abstract

Federated Learning (FL) has emerged as a promising paradigm in which multiple clients collaboratively train a shared global model while preserving data privacy. To create a robust and practical FL framework, it is crucial to extend its ability to generalize well to unseen domains - a problem referred to as federated Domain Generalization (FDG), being still under-explored. We propose an innovative federated algorithm, termed *hFedF* for *hypernetwork-based Federated Fusion*, designed to bridge the performance gap between generalization and personalization, capable of addressing various degrees of domain shift. Essentially, the hypernetwork supports a non-linear fusion of client models enabling a comprehensive understanding of the underlying data distribution. We encompass an extensive discussion and provide novel insights into the tradeoff between personalization and generalization in FL. The proposed algorithm outperforms strong benchmarks on three widely-used data sets for DG in an exceeding number of cases.

1. Introduction

Federated Learning (FL) has arisen as a beacon of innovation, particularly in its promise to harness decentralized data while upholding the sanctity of privacy (McMahan et al., 2016). In general, FL bridges data protection and performance deficiencies well. However, a far-reaching challenge of FL is that its performance degrades in cases where the data is not independently and identically distributed (i.e., *non-iid*) across the clients. This approach is particularly pivotal in domains where data confidentiality is paramount. For instance, in the realm of healthcare, institutions maintain ML applications for medical imaging and genetic analysis (Rieke et al., 2020; Prayitno et al., 2021). As the institutions

¹Department of Computer Science, Swiss Institute of Technology (ETH Zurich), Zurich, Switzerland ²KAIST AI, Seoul, South Korea. Correspondence to: Marc Bartholet <mob.ch@gmx.ch>.

Preprint.

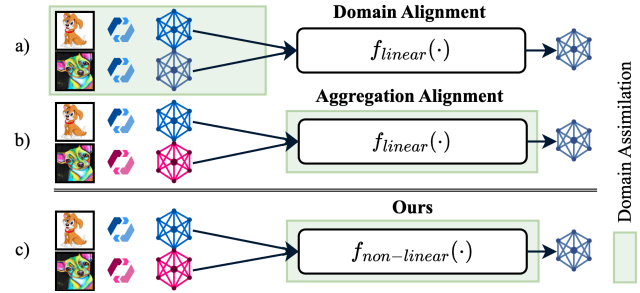


Figure 1. An overview of FDG Approaches: **a)** Conventional methods extract domain-invariant features during local model training (i.e., domain alignment). **b)** Standard approaches aggregate these models linearly for a generalized global model (i.e. aggregation alignment). **c)** Our method utilizes a non-linear hypernetwork to fuse local representations, enhancing both personalization and generalization capabilities.

collect highly sensitive patient data, they suffer individually from domain-biased data sets (Roth et al., 2023). Further, autonomous driving systems rely on robust object detection and must contend with domain variations due to heterogeneous weather conditions (Kim et al., 2023; Su et al., 2023). To preserve data security, collaboration on applications through FL would be beneficial, but the domain heterogeneity in the underlying data incurs existential performance issues (Li et al., 2023).

The divergence in domain-specific data, termed as *domain shift*, poses a formidable challenge. Federated Domain Generalization (FDG) specifically aims to address these shifts by enabling FL systems to generalize effectively to unseen domains. Traditional DG strategies, largely effective in centralized settings, struggle in FL due to their reliance on simultaneous access to all domains, a condition not feasible in distributed environments (Zhang et al., 2023b). Current efforts in FDG, such as those depicted in Figure 1a), concentrate on *federated domain alignment*, attempting to mitigate domain shifts by finding domain-invariant representations during local training. This endeavor has been approached through various methodologies, including adversarial training (Wang et al. (2022); Peng et al. (2019); Zhang et al. (2023a)) and regularization techniques (Zhang & Li (2022); Nguyen et al. (2022)). In parallel, others have tackled the

problem at the aggregation stage by aligning the weights to reflect the different domains (Yuan et al., 2023; Chen et al., 2022; Yang et al., 2023; Zhang et al., 2023b) (i.e. *aggregation alignment* Figure 1b). Yet, FDG remains an area ripe for innovative solutions.

Present FDG methods typically focus on linear aggregation strategies (i.e. weight averaging) to synthesize a generalizable global model from local updates, aiming to optimize contributions from varied domains. However, these approaches tend to underrepresent the multivariate¹ nature of domain shifts (Bai et al., 2023; Li et al., 2023), often reducing the complexity of local representations. This simplification can inadvertently diminish the in-distribution (*id*) performance for the sake of out-of-distribution (*ood*) generalization, leading to a trade-off that might not be necessary with more sophisticated approaches.

This paper presents a paradigm shift in FDG strategies by introducing a hypernetwork based non-linear aggregation framework that exploits collective knowledge through adaptive parameter-sharing (Figure 1c). Hypernetwork (Ha et al., 2016) is a Neural Network (NN) that takes a unique client embedding as input and generates parameters for the client model. Under our framework, the client weight parameters are implicitly shared using a hypernetwork (i.e. non-linear fusion function $f_{non-linear}(\cdot)$ in Figure 1c) that generates a quasi-global model for all clients. While federated hypernetworks have been proven under certain problem conditions (e.g., label heterogeneity, personalization) (Shamsian et al., 2021; Scott et al., 2023; Ma et al., 2022; Lin et al., 2023), this is the first work, to our best knowledge, that utilizes a hypernetwork approach in FDG. Our key contributions include:

- **Non-linear Aggregation:** We introduce a novel aggregation framework that enhances the balance between *id*- and *ood*-performance, utilizing non-linear fusion to cater to personalization and generalization. We leverage client-specific embeddings within a hypernetwork to improve the model’s performance without compromising data privacy (Section 3).
- **Strategic Domain Assignment:** Our method implicitly controls domain shift severity, simplifying the robustness across diverse domain (Section 4).
- **Empirical Validation:** We demonstrate improved performance on challenging multi domain datasets (PACS (Li et al., 2017b), Office-Home (Venkateswara et al., 2017), and VLCS (Fang et al., 2013)) under federated scenarios, validating our approach against existing benchmarks (Section 4).

¹Domain shifts can originate from various aspects of images features, e.g. color, resolution, or general depiction of objects.

- **Reliable Uncertainty Estimation:** Our method inherently provides reliable uncertainty estimation, naturally reducing confidence in incorrect predictions, which is critical for trustworthy applications (Section 5).
- **Analysis on Aggregation:** We conduct an in-depth analysis contrasting general linear weight averaging with our hypernetwork approach, revealing insights into the training dynamics (Section 5).

2. Related Work

2.1. Federated Learning

The objective of *FedAvg* is to train a single global model shared with all clients by averaging the all clients’ weight parameters (McMahan et al., 2016). Despite its simplicity, *FedAvg* is effective and still serves as a benchmark for most state-of-the-art FL algorithms. This holds especially for algorithms aiming for a high generalization performance (Bai et al., 2023) due to *FedAvg*’s smooth loss landscape (Qu et al., 2023; Lin et al., 2021). A common issue of applying *FedAvg* in the presence of *non-iid* data is that the average of the clients’ local optima drifts away from the global optima. As a result, there have been many attempts to minimize the drift by regularizing either the local or global update (Acar et al., 2021; Wang et al., 2020). *FedProx* (Li et al., 2020) proposes a lightweight modification to *FedAvg* by adding a L_2 regularization term to the local loss. Further, Karimireddy et al. (2021) introduces global and local control variates as estimates for the update directions of the server and the client, respectively.

2.2. Domain Generalization

In the field of non-federated DG, many techniques have been contributed with impressive results, such as domain alignment (Li et al., 2018), meta-learning (Li et al., 2017a), and regularization strategies (Wang et al., 2019), to name a few (Zhou et al., 2022; Li et al., 2023). Despite the promising studies, they can not be easily adapted to a FL setup. Nevertheless, recently there have been efforts that can be applied to FDG. One of the first algorithms, FedDG (Liu et al., 2021), involves an exchange of image distributions from the frequency space across clients together with an explicit regularization to promote domain-independent feature cohesion. Wang et al. (2022); Peng et al. (2019); Zhang et al. (2023a) use adversarial training techniques. *FedSR* (Nguyen et al., 2022) introduced two regularizers in order to enforce probabilistic feature representations of data samples from different domains. (Yuan et al., 2023; Chen et al., 2022; Yang et al., 2023; Zhang et al., 2023b) optimize the allocation of aggregation weights that allow for the efficient assimilation of contributions from isolated domains. *FedGMA* (Tenison et al., 2022) implicitly adjusts

the aggregation weights and Tian et al. (2023) aligns the local gradients to identify consistent patterns shared among clients.

2.3. Hypernetwork

Hypernetworks (a.k.a. meta-networks) (Ha et al., 2016) have gained attention in the field of multi-domain learning (Volk et al., 2022; Qu et al., 2023; Mahabadi et al., 2021) to facilitate joint learning by sharing knowledge across domains. *HMOE* (Qu et al., 2023) proposes a hypernetwork-based Mixture of Experts for DG that learns the embedding space of the input and minimizes the divergence between the predicted and already established embeddings. The idea of using hypernetworks within a federated framework is relatively new, with only a limited number of studies on this topic. Inspired by prior experience of hypernetworks in a centralized setup, Shamsian et al. (2021) releases with *pFedHN* the first hypernetwork-based alternative to established FL techniques. Conditioned on a client embedding, the hypernetwork outputs asynchronously client-specific parameters. Ma et al. (2022) makes use of a hypernetwork in a different way. Their hypernetwork outputs a weight matrix for each client used to identify the mutual contribution at layer granularity. To our best knowledge, all other works (Lin et al., 2023; Scott et al., 2023) have claimed hypernetworks for the generation of highly personalized models while neglecting domain shifts.

3. Method

3.1. Preliminaries

The generic FL setup can be stated as follows:

Definition 3.1. Let N be the number of clients participating in the learning system. Each client i has a data distribution, which is sampled from a distribution family $\mathcal{P}_i \sim \mathcal{B}$ and is defined over the same feature \mathcal{X} and label space \mathcal{Y} , i.e. $\mathcal{P}_i : \mathcal{X} \times \mathcal{Y} \rightarrow [0, 1]$, where $\mathcal{X} \times \mathcal{Y} = \{(x, y) \mid x \in \mathcal{X}, y \in \mathcal{Y}\}$. A client having access to its personal joint data distribution $\mathcal{P}_i(X, Y)$, samples thereof its data set $\mathcal{D}_i = \{(x_i^j, y_i^j)\}$. This local data set \mathcal{D}_i is used by the client to train its local ML model \mathcal{M}_i with parameters φ_i .

FL can be formulated as an optimization problem by minimizing the global objective function:

$$\min_{\{\varphi_i\}_{i=1}^N} \left\{ \mathcal{L}(\{\varphi_i\}_{i=1}^N) := \frac{1}{\sum_i \gamma_i} \sum_{i=1}^N \gamma_i \mathcal{L}_i(\varphi_i) \right\} \quad (1)$$

It is the weighted average of the local objective functions. The local objective function can be stated as follows²:

²Since the underlying data distribution \mathcal{P}_i is usually unknown, the expected loss can be approximated by the empirical loss.

$$\mathcal{L}_i(\varphi_i) = \mathbb{E}_{x, y \sim \mathcal{P}_i} [\ell_i(y; x, \varphi_i)] \quad (2)$$

$$\approx \frac{1}{|\mathcal{D}_i|} \sum_{j=1}^{|\mathcal{D}_i|} \ell_i(y_i^j; x_i^j, \varphi_i), \quad (3)$$

where $\ell_i : \mathcal{Y} \times \mathcal{Y} \rightarrow \mathbb{R}_+$ is the local loss function.

3.2. Problem Formulation

The proposed algorithm should not only minimize the expected loss on the data distributions seen in the FL training process, i.e. maximizing *id*-accuracy, but also on an unseen data distribution of a target domain \mathcal{S}_{trg} , i.e. maximizing *ood*-accuracy. FDG can be defined as follows:

Definition 3.2. In FDG, the clients are given a set of $K - 1$ source domains $\mathcal{Z}_{src} = \{Z_i\}_{i=1}^{K-1}$ and a target domain $\mathcal{Z}_{trg} = \{Z_K\}$, each associated with a domain shift wrt. to others. The marginal distributions $\mathcal{P}(X)$ between each pair of domains are different, $\mathcal{P}_i(X) \neq \mathcal{P}_j(X)$ for any pair $i, j \in \{1, \dots, K\}$. The goal is to learn client models *only* using data of the source domains, i.e. \mathcal{Z}_{src} , during training such that the prediction error on the *unseen* target domain $\mathcal{Z}_{trg} = \{Z_K\}$ is minimized.

3.3. Motivation

A federated model that can adapt to an unknown target domain has many advantages. A domain-generalized model supports (1) fairness by suppressing the inherent bias in training data from a single domain; (2) robustness by responding well to unseen changes, such as noisy data, outliers, and new domains; and (3) efficiency by reducing resources of domain-specific training.

In general, DG is a major challenge because the domain shifts are multifaceted and the target distribution is unknown. When DG faces FL, the difficulty is even greater as the data of the source domains may not be shared. Consequently, a highly generalizable model must be distilled only from the latent representations of the client models. At this point, the previous linear aggregation scheme reaches its limits, as it is unable to capture the complex distribution shifts. For this reason, we have developed a federated architecture that uses a hypernetwork as a non-linear aggregator. Compared to current hypernetwork approaches in FL, we are the first to promote the generation of a converging global model and synchronous updates. Table 1 summarizes how our hypernetwork distinguishes itself from the previous ones.

3.4. Algorithm

At each communication round, the hypernetwork on the server generates and subsequently distributes the model

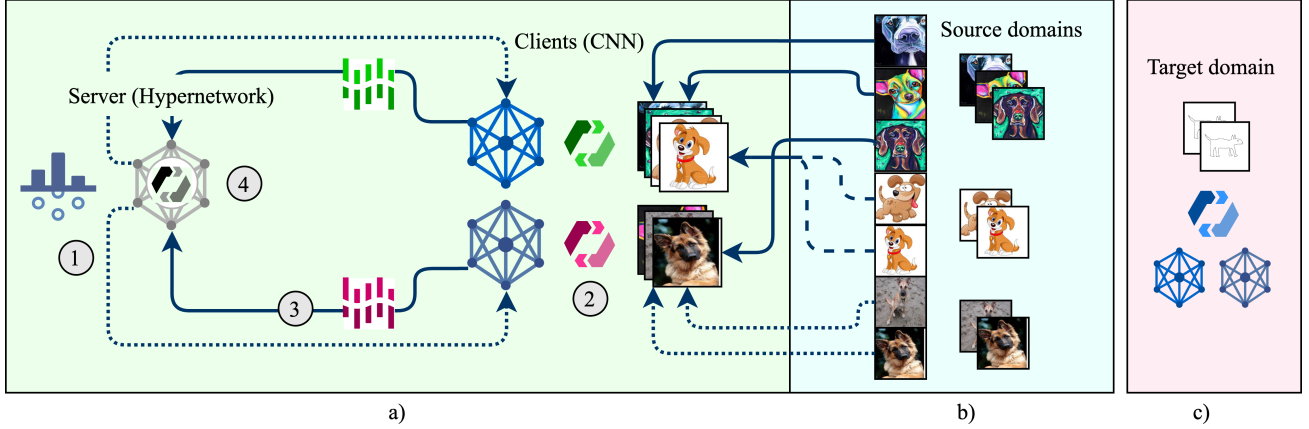


Figure 2. **a)** Proposed framework of the federated training with source domains - described in Section 3.4. **b)** Proposed strategy to split the source domains among the clients: The case of splitting 3 domains across 2 clients is visualized, where each client holds samples from 2 domains, i.e. $d = 2$. The top domain has the most samples and is therefore split into one more part than the other two domains to fulfill the given constraints. **c)** At inference, the generalization performance of the client models is evaluated on an unseen target domain and the personalization performance on a held-out subset of the local data sets consisting of source domains, according to (2).

Table 1. Comparison of literature’s and our hypernetwork.

CHARACTERISTICS	LITERATURE	OURS
CONVERGING CLIENTS	×	✓
SYNCHRONOUS UPDATE	×	✓
LEARNABLE EMBEDDING	✓	✓
FDG	×	✓

states for each client (1 in Figure 2). The clients update their models individually for a certain amount of iterations using their local data. After the local update is completed, the clients approximate the gradients wrt. their model parameters by taking the difference between the updated state and the one initially received from the server (2 in Figure 2). Next, the clients communicate synchronously the approximated gradient to the server (3 in Figure 2). The server computes the update direction of the hypernetwork based on the proposed gradient estimates of the clients and aggregates the individual gradients using a weighted average. The weight connected to a gradient positively correlates with its similarity to the dominant (averaged) update direction. Lastly, the server performs a single update step on the hypernetwork along the proposed direction and smooths it by factoring in a short-term average of the model state (4 in Figure 2).

3.4.1. HYPERNETWORK-GENERATED MODELS

An advantage of using hypernetworks for FL is that the communication costs only depend on the number of parameters of the target network, allowing the server-side system to have arbitrary model complexity without incurring higher communication costs. In addition, our hypernetworks pro-

vides a high degree of privacy. First, the misappropriation of a client model does not straightaway reveal the models of all other participants in the system due to the marginal personalization of models. Second, the embeddings learned by the hypernetwork always remain on the server and are never communicated. Moreover, they are not human-interpretable, i.e., they do not trivially reveal information about the clients and their data. Remarkably, we show in Appendix A.1.4, that a randomization of our embeddings achieve comparable performance while guaranteeing higher privacy standards.

The hypernetwork \mathbf{h} , parameterized by θ , learns the embedding space $\nu \in \mathbb{R}^{e \times N}$ of the clients. It takes the client ID i as an input and outputs client-specific parameters φ_i for client i .

$$\varphi_i = \mathbf{h}(i; \theta, \nu), \text{ where } \nu = [\nu_1, \dots, \nu_i, \dots, \nu_N]^T \quad (4)$$

The global optimization problem by means of a hypernetwork for the proposed algorithm then becomes:

$$\min_{\theta, \nu} \left\{ \mathcal{L}(\theta, \nu) := \frac{1}{\sum_i \gamma_i} \sum_{i=1}^N \gamma_i \mathcal{L}_i(\mathbf{h}(i; \theta, \nu)) \right\} \quad (5)$$

The hypernetwork and the embedding can be trained using differential computation in an extended chain-rule fashion. The gradients of the loss of the client model wrt. all its parameters (1 in Equation 6) are propagated back to the gradients of the parameters of the hypernetwork (2 in Equation 6). The gradients wrt. the parameters of the hypernetwork $\nabla_{\theta, \nu} \mathcal{L}_i$ are then obtained by applying the chain rule as follows:

$$\nabla_{\theta, \nu} \mathcal{L}_i(\varphi_i) = \underbrace{\nabla_{\theta, \nu} \varphi_i^T}_{(2)} \cdot \underbrace{\nabla_{\varphi_i} \mathcal{L}_i(\varphi_i)}_{(1)} \quad (6)$$

Algorithm 1 *hFedF* (Federated Training)

Require: T - number of communication rounds, E - number of local epochs, α - server's learning rate, μ - clients' learning rate, \mathcal{D}_i - local data of client i , \mathcal{S} - set of clients

Initialize: θ^0, ν^0

for $t \in \{0, \dots, T\}$ **do**

compute $\varphi_i^t \leftarrow h(\theta^t, \nu^t)$ for client $i \in \mathcal{S}$

communicate φ_i^t to client $i \in \mathcal{S}$

for each client $i \in \mathcal{S}$ **in parallel do do**

initialize $\tilde{\varphi}_i^t \leftarrow \varphi_i^t$

for $e \in \{1, \dots, E\}$ **do**

$\tilde{\varphi}_i^t \leftarrow \mathbf{ClientUpdate}(\tilde{\varphi}_i^t; \mathcal{D}_i, \mu)$

end for

$\Delta\varphi_i^t \leftarrow \tilde{\varphi}_i^t - \varphi_i^t$

communicate $\Delta\varphi_i^t$ to server

end for

$g_i^t \leftarrow \nabla_{\theta, \nu} \varphi_i^{T, t} \cdot \Delta\varphi_i^t$ for client $i \in \mathcal{S}$

$\tilde{\gamma}_i^t \leftarrow \mathbf{GradAlign}(g_i^t, \mathcal{S})$ // Eq. 8 & 9

$g^t \leftarrow \sum_{i \in \mathcal{S}} \tilde{\gamma}_i^t \cdot g_i^t$

$\{\theta^{t+1}, \nu^{t+1}\} \leftarrow \{\theta^t, \nu^t\} - \alpha \cdot g^t$

$\{\theta^{t+1}, \nu^{t+1}\} \leftarrow \mathbf{EMA}(\{\theta^{t+1}, \nu^{t+1}\}, t)$ // Eq. 10

end for

Return server: θ, ν

Return client i : φ_i

And, by the linearity of differentiation, the derivative of the linear combination of losses \mathcal{L}_i equals the linear combination of the derivatives of the losses \mathcal{L}_i . From that follows the server-side aggregation of the client gradients $\nabla \mathcal{L}_i$, where the weights γ_i are a design choice.

$$\nabla \mathcal{L} = \nabla \frac{1}{\sum_i \gamma_i} \sum_{i=1}^N \gamma_i \mathcal{L}_i = \frac{1}{\sum_i \gamma_i} \sum_{i=1}^N \gamma_i \nabla \mathcal{L}_i \quad (7)$$

However, to increase the communication efficiency and the convergence speed, multiple gradient steps are executed on the client side during each communication round (McMahan et al., 2016). The personalized parameters φ_i received from the hypernetwork are subjected to several local optimization steps to obtain $\tilde{\varphi}_i$. Thereby, the local gradient $\nabla_{\varphi_i} \mathcal{L}_i$ is approximated by computing the difference $\Delta\varphi_i := \tilde{\varphi}_i - \varphi_i$. This approximation is inspired by the work of Zhang et al. (2019).

3.4.2. GRADIENT ALIGNMENT

Due to the hypernetwork's inherent flexibility, the competition among clients can potentially undermine the global objective. Given that the hypernetwork outputs parameters tailored for handling diverse data distributions, its updates on the server may suffer from divergent gradients. Since all clients contribute to the shared hypernetwork, the gradient

introduced by one client ultimately affects all others. For instance, a client dealing with an outlying data distribution can indirectly impede the optimal solutions of other clients. This, in turn, can result in slow, unstable, and potentially sub-optimal convergence within the federated system.

To mitigate *client drift*, this work introduces a novel, non-parametric gradient alignment technique to the aggregation. Initially, the server applies for each approximate gradient $\Delta\varphi_i$, transmitted by client i , the chain rule to obtain the proposed update direction g_i according to Equation 6. Then, the server calculates the average update direction g_{avg} from all clients. Subsequently, the alignment of each gradient g_i with the average direction g_{avg} is assessed using cosine similarity. This yields the preliminary aggregation weights γ_i .

$$\gamma_i = \frac{g_{\text{avg}} \cdot g_i}{\|g_{\text{avg}}\| \|g_i\|}, \text{ where } g_{\text{avg}} = \frac{1}{N} \sum_{i=1}^N g_i \quad (8)$$

To attain a well-defined discrete probability distribution over all weights, the *softmax* function is applied, yielding the final weights.

$$\tilde{\gamma}_i = \frac{e^{-\gamma_i}}{\sum_{j=1}^N e^{-\gamma_j}} \quad (9)$$

The final hypernetwork gradient is then determined through a linear combination of local gradients, taking into account the previously calculated weights. Notably, we analyze the convergence of the aggregation weights and discuss their final distribution in Appendix A.1.1. A direct comparison of the performance of *hFedF* with and without GradAlign is also conducted in Appendix A.1.2 to showcase its benefit.

3.4.3. EMA REGULARIZATION

Hypernetworks can encounter numerical stability issues (Chauhan et al., 2023). To ensure the stability of the hypernetwork training, periodic regularization is applied using an EMA. Mathematically, the exponentially smoothed model θ_{EMA}^t is computed as a weighted average of the currently observed model θ^t and the previously smoothed model $\theta_{\text{EMA}}^{t-1}$. Over time, the smoothed model becomes a weighted average of increasing past observations, favoring more recent model states.

$$\theta_{\text{EMA}}^t = \alpha\theta^t + (1 - \alpha)\theta_{\text{EMA}}^{t-1} \quad (10)$$

We choose α to be close to 1 to maintain the responsiveness to recent changes and reduce the sensitivity to the initialization of the EMA. Additionally, we initialize the moving average with a model state after several communication rounds. This bypasses bad initialization during the unstable early phase of training. Furthermore, the effect of EMA is visualized in Appendix A.1.8 and its added value to the performance of *hFedF* is evaluated in A.1.2.

4. Experiments

4.1. Setup

The experimental data setup adheres to the guideline of *DomainBed* (Gulrajani & Lopez-Paz, 2020). This paper opts for a leave-one-domain-out validation approach, where all domains but one are used as source domains for training $\mathcal{Z}_{\text{src}} = \{\mathcal{Z}_k\}_{k=1}^{K-1}$ and the remaining domain as target domain $\mathcal{Z}_{\text{trg}} = \{\mathcal{Z}_K\}$. Notably, for each client i , a fraction (10%) of its source domains is held out as validation set $\mathcal{D}_{i,\text{val}}$ to measure the *id*-accuracy (personalization performance). The data from the target domain $\mathcal{D}_K = \mathcal{D}_{\text{test}}$ is used to evaluate the *ood*-accuracy (generalization performance). In this study, we set N equal to the number of source domains $|\mathcal{Z}_{\text{src}}|$. As said to be optimal by Shamsian et al. (2021), the embedding dimension e is subsequently set to $\lfloor 1 + \frac{N}{4} \rfloor$. However, results with higher embedding dimensions and more clients are presented in Appendix A.1.3 and A.1.5, respectively.

Moreover, we propose a novel strategy for allocating different domains to clients to address the challenge of managing the degree of domain shift. This strategy is developed to ensure transparency and efficiency in its implementation and subsequent application. It allows to split any number of source domains into any number of clients, solely based on the hyperparameter d . This hyperparameter specifies each client’s distinct domains in its training data. At a high level, the process involves partitioning each domain and subsequently distributing these partitions to the clients based on the selected value of d .

The three data sets used for evaluation are PACS (Li et al., 2017b), Office-Home (Venkateswara et al., 2017), and VLCS (Fang et al., 2013). Although they have each 4 domains, they exhibit an increasing classification difficulty due to their number of classes and domain representations.

Following related works (Shamsian et al., 2021; Qu et al., 2023; Chen & Chao, 2022; Volk et al., 2022; von Oswald et al., 2022; Henning et al., 2021), we choose the model of the hypernetwork to be a Multi-Layer Perceptron. The architecture comprises an embedding layer followed by three hidden layers, each containing 50 neurons. Crucially, the network terminates with a multi-head structure, each head being another linear layer that maps to the dimensions of a single layer of the client model. To have a high-performing client model, we designed a Convolutional NN whose architecture avoids undesirable computational complexities and excessive memory consumption.

We compare our proposed method - *hFedF* - thoroughly against a diverse set of benchmark algorithms. The selected benchmarks all tackle *non-iid* data setups in FL from different angles and jointly intend to give a comprehensive assessment of the current FL abilities in the presence of

domain shift ([*FedAvg*, *FedProx*, *pFedHN*] for *non-iid* data and [*FedSR*, *FedGMA*] for FDG). In addition, to understand the strengths and weaknesses of FL, two non-federated approaches are also evaluated. *Central* describes the setup where the domains are centrally stored and trained on a single model. *Local* distributes the domains across the clients. However, no communication takes place.

All combinations of source and target domains are considered. The results are reported for each data set separately, reflecting the average performance across all target domains \mathcal{Z}_{trg} within the cross-validation. Additionally, the experiments are averaged across three seeds for enhanced consistency. All algorithms are trained with the same model on the client side. Moreover, each algorithm is executed for 200 communication rounds. During each round, the client is updated for 2 local epochs using a batch size of 64. Additionally, their hyperparameters are tuned per data set in line with reference papers. Notably, the detailed results, separated by domain, can be found in Appendix A.3, and more details about the experimental setup in A.2. In particular, the rationale behind the number of epochs is discussed in Appendix A.1.6 and the long-term behavior - after 200 communication rounds - illustrated in A.1.7.

4.2. Results

The best accuracy along a column is marked in **bold**, with the exception of non-federated benchmarks. The proposed algorithm consistently outperforms most FL benchmarks in terms of *id*- and *ood*-accuracy across various data sets and task difficulties. The algorithm demonstrates significant improvements in generalization performance, particularly in handling extreme domain shifts ($d = 1$), with margins of 3.3% on PACS. Regarding personalization performance, the presented algorithm still surpasses other FL methods by 1.4% on PACS. However, when evaluated on VLCS with one source domain per client ($d = 1$), the algorithm falls slightly short of other benchmarks.

In contrast, when a client encounters more than one source domain during training ($d > 1$), our proposed method emerges as the overall best-performing. Moreover, the presented algorithm effectively utilized the hypernetwork and drastically improves over the pioneering work *pFedHN* (e.g., +3.9% *id*-accuracy and +4.9% *ood*-accuracy on PACS). The marginal performance improvements with increasing d suggest that the leave-one-domain-out validation strategy in DG is inherently challenging. Applying FL is worthwhile - the proposed algorithm excels the personalization and generalization performances of the *Local* method in almost every case and of the *Central* method even in every case. It can be observed that *FedAvg* is a strong benchmark even though it was not explicitly designed for DG, substantiating the remarks in 2.1. The VLCS data set offers the biggest

challenges, possibly due to its photo-realistic images, which makes classification less straightforward compared to the PACS and Office-Home data sets.

Table 2. Averaged accuracy across domains on PACS.

	$d = 1$		$d = 2$		$d = 3$	
	μ_{id}	μ_{ood}	μ_{id}	μ_{ood}	μ_{id}	μ_{ood}
CENTRAL	-	-	-	-	75.4	53.7
LOCAL	76.4	35.8	71.5	43.3	69.6	45.9
FEDAVG	70.1	51.3	75.5	53.2	76.9	53.5
FEDPROX	69.9	50.7	75.1	53.0	77.3	53.8
pFEDHN	65.2	48.2	72.2	50.6	74.3	51.1
FEDSR	69.2	48.9	73.8	51.6	75.8	52.2
FEDGMA	68.7	48.9	70.6	49.9	72.7	49.9
hFEDF	71.5	54.6	75.8	54.9	76.1	55.2

Table 3. Averaged accuracy across domains on Office-Home.

	$d = 1$		$d = 2$		$d = 3$	
	μ_{id}	μ_{ood}	μ_{id}	μ_{ood}	μ_{id}	μ_{ood}
CENTRAL	-	-	-	-	49.5	28.1
LOCAL	47.7	17.2	40.5	19.7	36.9	20.8
FEDAVG	47.8	29.1	51.3	29.4	51.7	29.4
FEDPROX	48.6	29.1	51.5	29.7	51.8	29.9
pFEDHN	49.9	21.1	45.1	23.6	44.0	25.8
FEDSR	48.1	29.6	51.5	29.8	52.0	30.2
FEDGMA	47.7	29.5	51.4	30.0	51.7	29.6
hFEDF	49.4	29.8	52.1	31.2	52.2	31.7

Table 4. Averaged accuracy across domains on VLCS.

	$d = 1$		$d = 2$		$d = 3$	
	μ_{id}	μ_{ood}	μ_{id}	μ_{ood}	μ_{id}	μ_{ood}
CENTRAL	-	-	-	-	62.8	55.8
LOCAL	69.9	43.6	63.2	50.0	58.8	51.6
FEDAVG	65.6	58.0	65.6	57.7	65.3	57.4
FEDPROX	65.4	56.2	64.6	56.7	65.2	56.2
pFEDHN	63.4	56.2	63.9	57.0	64.3	57.0
FEDSR	66.0	57.2	65.2	57.4	65.1	57.5
FEDGMA	66.4	57.2	65.6	56.7	65.3	57.2
hFEDF	66.1	56.9	66.8	58.1	65.7	58.7

5. Discussion

5.1. Uncertainty Estimator

The critical question remains why the proposed algorithm generalizes superior to other strong benchmarks — two main indicia reason on the underlying workings. Upon closer examination of the inference landscape, it becomes

evident that the proposed algorithm serves as a more reliable uncertainty estimator. Essentially, it possesses a deeper understanding of its predictive capabilities and is less overconfident than other FL algorithms. This explanation is supported by the insights of Figure 3. Our algorithm demonstrates confidence in its correct predictions, comparable to other benchmarks. Conversely, regarding incorrect predictions, it is aware of its potential errors and expresses the uncertainty through lower probability values assigned to the predicted class. Lin et al. (2021); Tenison et al. (2022) attributed the high prediction uncertainty of *FedAvg* to its soft decision boundaries. This could indicate that we are able to further optimize the smoothing of decision boundaries by integrating a hypernetwork-based extension of complexity into our architecture. This allows us to capture the relationships and underlying patterns in the feature space more robustly. Notably, the FL algorithms, i.e., *FedAvg* and *hFedF*, are generally less certain about their predictions if the sample is *ood*. This aligns with the expectation that predictions of unseen domains should carry a higher uncertainty.

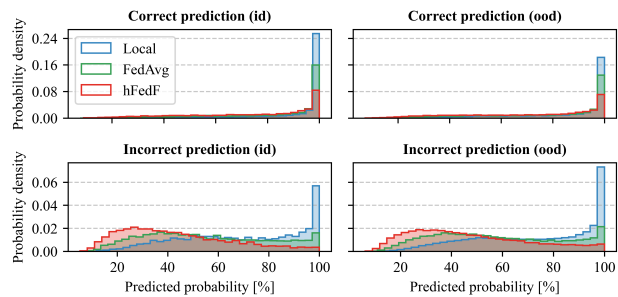


Figure 3. Histogram of the probability of predicted class. *Office-Home*, $d = 1$. For ease of comparison, the *Local* method is included due to its poor performance. In addition, *FedAvg* is selected due to its good reception in literature and robust performance.

5.2. Client Embedding

The learned client embeddings offer another perspective on the outstanding generalization performance of the proposed algorithm. In Figure 4, each subplot depicts the 1-dimensional client embedding, learned by the hypernetwork, depending on how the source domains are distributed among the clients. Remarkably, only minor differences are observed between the embedding spaces within each subplot. Apparently, the embeddings depend solely on the left-out target domain. It can be concluded that the hypernetwork gains a thorough understanding of the overall data distribution present in the federated system - irrespective of how the data is distributed. However, it is crucial to note that the client embeddings do not converge into a single one. This aspect could serve as an additional argument for the great awareness regarding its predictive capabilities. Unlike *FedAvg*, it may comprehend the underlying data distribution

more sophisticatedly. The hypernetwork still incorporates a low degree of parameters-sharing beneath the surface to overcome the challenges of DG. Moreover, to offer a substantiated explanation regarding the significance of the client embeddings and their contribution to an enhanced data privacy of the proposed method, we examine its significance in more detail in A.1.3 and A.1.4, respectively.

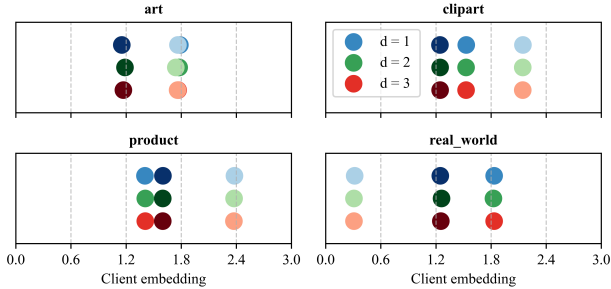


Figure 4. The learned client embeddings are one-dimensional. The different colors symbolizes different allocation of domains per client and the color shades mark the different clients. *Office-Home*.

5.3. Non-linear Fusion

In summary, it can be stated that the hypernetwork produces a quasi-global model, with marginal variations among the clients. This behavior can be verified by Figure 5 which contrast the model variations of the proposed method against only locally trained client models. It opts to function as an effective generalizer without sacrificing personalization performance.

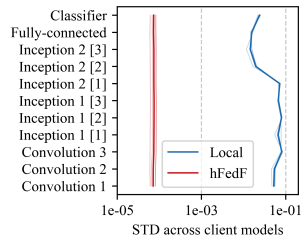


Figure 5. Differences between client models. The standard deviation is calculated based on the distribution of model weights sampled from all clients. For each layer, the standard deviation is averaged across all parameters within that layer. *PACS*; $d = 1$.

Through a detailed examination of the computational flow of our proposed hypernetwork approach, it can be asserted that it fundamentally operates as a non-linear aggregation scheme. This distinguishes it from conventional methods like *FedAvg*. The introduced non-linearity enables a nuanced understanding of the data distribution within the federated framework, leading to exceptional performance, especially in the presence of domain shifts. The hypernetwork tends to share knowledge between clients more effectively than other present FL algorithms.

In generic FL algorithms (Equation 11), the updated global model φ can be viewed as a linear function of the locally

updated models $\tilde{\varphi}_i$.

$$\varphi^{t+1} = f_{\text{lin}}(\cdot) \approx \varphi^t + \alpha \cdot \sum_{i=1}^N \tilde{\varphi}_i^t - \varphi^t \quad (11)$$

For illustrative purposes and following the observation of converging clients, the proposed method has been simplified to generate a single global model φ^t at time t . Further, α is a design choice of the specific FL algorithm. The non-linearity of the proposed method emerges from the non-linear NN, being the hypernetwork \mathbf{h} (Equation 12). In Equation 12, the notation is abused for easier comparison to Equation 11.

$$\varphi^{t+1} = f_{\text{non-lin}}(\cdot) \approx \mathbf{h}(\theta - \alpha \cdot \sum_{i=1}^N \nabla_{\theta}(\tilde{\varphi}_i^t, \varphi^t)) \quad (12)$$

5.4. Limitations and Future Work

Regrettably, the current implementation faces scalability issues when using complex state-of-the-art vision models. The hypernetwork would be required to predict millions of parameters. This leads to high convergence instability and memory demands mainly due to the last layer of the hypernetwork. Compared to other benchmark algorithms, the current setup places additional computational strain on the server due to the hypernetwork updates. However, this added workload is considered nearly negligible because the server is expected to have ample resources to update a single model during each communication round. Nevertheless, our method could be extended to more *non-iid* problems due to its promising ability to understand complex data distributions. Other future research can be outlined by adapting our framework to be compatible with large pretrained vision models. Possible avenues for extending research, with the goal of addressing scalability constraints, could involve applying the hypernetwork only to a subset of layers or utilizing it as a fine-tuning tool.

6. Conclusion

In conclusion, this paper encourages a non-linear aggregation scheme resulting in a FL method with a robust ability to tradeoff between generalizing and personalizing. The method we propose provides a conceptual advancement of hypernetwork research in FL and introduces it to the challenging field of DG. Despite its drawback of scalability, the method provides a promising answer to the addressed research questions and demonstrates a comprehensive understanding of managing diverse data distributions in FL. Positioned within a novel research direction, it stands ready for further extension to other practical settings in FL.

Impact Statement

This paper presents work whose goal is to advance the field of Machine Learning. There are many potential societal consequences of our work, none which we feel must be specifically highlighted here.

References

- Acar, D. A. E., Zhao, Y., Navarro, R. M., Mattina, M., Whatmough, P. N., and Saligrama, V. Federated Learning Based on Dynamic Regularization, 2021.
- Bai, R., Bagchi, S., and Inouye, D. I. Benchmarking Algorithms for Federated Domain Generalization, 2023.
- Chauhan, V. K., Zhou, J., Lu, P., Molaei, S., and Clifton, D. A. A Brief Review of Hypernetworks in Deep Learning, 2023.
- Chen, H.-Y. and Chao, W.-L. On Bridging Generic and Personalized Federated Learning for Image Classification, 2022.
- Chen, J., Li, J., Huang, R., Yue, K., Chen, Z., and Li, W. Federated Transfer Learning for Bearing Fault Diagnosis With Discrepancy-Based Weighted Federated Averaging. *IEEE Transactions on Instrumentation and Measurement*, 71:1–11, 2022. doi: 10.1109/TIM.2022.3180417.
- Fang, C., Xu, Y., and Rockmore, D. N. Unbiased Metric Learning: On the Utilization of Multiple Datasets and Web Images for Softening Bias. *2013 IEEE International Conference on Computer Vision*, pp. 1657–1664, 2013.
- Gulrajani, I. and Lopez-Paz, D. In Search of Lost Domain Generalization, 2020.
- Ha, D., Dai, A., and Le, Q. V. HyperNetworks, 2016.
- Henning, C., Cervera, M. R., D’Angelo, F., von Oswald, J., Traber, R., Ehret, B., Kobayashi, S., Grewe, B. F., and Sacramento, J. Posterior Meta-Replay for Continual Learning, 2021.
- Karimireddy, S. P., Kale, S., Mohri, M., Reddi, S. J., Stich, S. U., and Suresh, A. T. SCAFFOLD: Stochastic Controlled Averaging for Federated Learning, 2021.
- Kim, T., Lin, E., Lee, J., Lau, C., and Mugunthan, V. Navigating data heterogeneity in federated learning: A semi-supervised approach for object detection. In *Thirty-seventh Conference on Neural Information Processing Systems*, 2023.
- Li, D., Yang, Y., Song, Y.-Z., and Hospedales, T. M. Learning to Generalize: Meta-Learning for Domain Generalization, 2017a.
- Li, D., Yang, Y., Song, Y.-Z., and Hospedales, T. M. Deeper, Broader and Artier Domain Generalization, 2017b.
- Li, H., Pan, S. J., Wang, S., and Kot, A. C. Domain Generalization with Adversarial Feature Learning. In *2018 IEEE/CVF Conference on Computer Vision and Pattern Recognition*, pp. 5400–5409, 2018. doi: 10.1109/CVPR.2018.00566.
- Li, T., Sahu, A. K., Zaheer, M., Sanjabi, M., Talwalkar, A., and Smith, V. Federated Optimization in Heterogeneous Networks, 2020.
- Li, Y., Wang, X., Zeng, R., Donta, P. K., Murturi, I., Huang, M., and Dustdar, S. Federated Domain Generalization: A Survey, 2023.
- Lin, T., Kong, L., Stich, S. U., and Jaggi, M. Ensemble Distillation for Robust Model Fusion in Federated Learning, 2021.
- Lin, Y., Wang, H., Li, W., and Shen, J. Federated learning with hyper-network—a case study on whole slide image analysis. *Scientific Reports*, 13, 01 2023. doi: 10.1038/s41598-023-28974-6.
- Liu, Q., Chen, C., Qin, J., Dou, Q., and Heng, P.-A. FedDG: Federated Domain Generalization on Medical Image Segmentation via Episodic Learning in Continuous Frequency Space, 2021.
- Ma, X., Zhang, J., Guo, S., and Xu, W. Layer-wised Model Aggregation for Personalized Federated Learning. In *2022 IEEE/CVF Conference on Computer Vision and Pattern Recognition (CVPR)*, pp. 10082–10091, Los Alamitos, CA, USA, jun 2022. IEEE Computer Society. doi: 10.1109/CVPR52688.2022.00985.
- Mahabadi, R. K., Ruder, S., Dehghani, M., and Henderson, J. Parameter-efficient Multi-task Fine-tuning for Transformers via Shared Hypernetworks, 2021.
- McMahan, H. B., Moore, E., Ramage, D., Hampson, S., and y Arcas, B. A. Communication-Efficient Learning of Deep Networks from Decentralized Data, 2016.
- Nguyen, A. T., Torr, P., and Lim, S.-N. FedSR: A Simple and Effective Domain Generalization Method for Federated Learning. In Oh, A. H., Agarwal, A., Belgrave, D., and Cho, K. (eds.), *Advances in Neural Information Processing Systems*, 2022.
- PapersWithCode. Domain Generalization on Office-Home. <https://paperswithcode.com/sota/domain-generalization-on-office-home>, a. Accessed: 2024-02-01.

- PapersWithCode. Domain Generalization on PACS. <https://paperswithcode.com/sota/domain-generalization-on-pacs-2>, b. Accessed: 2024-02-01.
- PapersWithCode. Domain Generalization on VLCS. <https://paperswithcode.com/sota/domain-generalization-on-vlcs>, c. Accessed: 2024-02-01.
- Peng, X., Huang, Z., Zhu, Y., and Saenko, K. Federated Adversarial Domain Adaptation, 2019.
- Prayitno, Shyu, C.-R., Putra, K. T., Chen, H.-C., Tsai, Y.-Y., Hossain, K. S. M. T., Jiang, W., and Shae, Z.-Y. A Systematic Review of Federated Learning in the Healthcare Area: From the Perspective of Data Properties and Applications. *Applied Sciences*, 11(23), 2021. ISSN 2076-3417. doi: 10.3390/app112311191.
- Qu, J., Faney, T., Wang, Z., Gallinari, P., Yousef, S., and de Hemptinne, J.-C. HMOE: Hypernetwork-based Mixture of Experts for Domain Generalization, 2023.
- Rieke, N., Hancox, J., Li, W., Milletar, F., Roth, H. R., Albarqouni, S., Bakas, S., Galtier, M. N., Landman, B. A., Maier-Hein, K., Ourselin, S., Sheller, M., Summers, R. M., Trask, A., Xu, D., Baust, M., and Cardoso, M. J. The future of digital health with federated learning. *npj Digital Medicine*, 3(1), sep 2020. doi: 10.1038/s41746-020-00323-1.
- Roth, H. R., Cheng, Y., Wen, Y., Yang, I., Xu, Z., Hsieh, Y.-T., Kersten, K., Harouni, A., Zhao, C., Lu, K., Zhang, Z., Li, W., Myronenko, A., Yang, D., Yang, S., Rieke, N., Quraini, A., Chen, C., Xu, D., Ma, N., Dogra, P., Flores, M., and Feng, A. NVIDIA FLARE: Federated Learning from Simulation to Real-World, 2023.
- Scott, J., Zakerinia, H., and Lampert, C. H. PeFLL: A Lifelong Learning Approach to Personalized Federated Learning, 2023.
- Shamsian, A., Navon, A., Fetaya, E., and Chechik, G. Personalized Federated Learning using Hypernetworks, 2021.
- Su, S., Li, B., Zhang, C., Yang, M., and Xue, X. Cross-domain federated object detection. In *2023 IEEE International Conference on Multimedia and Expo (ICME)*. IEEE, July 2023. doi: 10.1109/icme55011.2023.00254.
- Szegedy, C., Liu, W., Jia, Y., Sermanet, P., Reed, S., Anguelov, D., Erhan, D., Vanhoucke, V., and Rabinovich, A. Going Deeper with Convolutions, 2014.
- Tenison, I., Sreeramadas, S. A., Mugunthan, V., Oyallon, E., Belilovsky, E., and Rish, I. Gradient Masked Averaging for Federated Learning, 2022.
- Tian, C. X., Li, H., Wang, Y., and Wang, S. Privacy-Preserving Constrained Domain Generalization via Gradient Alignment, 2023.
- Venkateswara, H., Eusebio, J., Chakraborty, S., and Panchanathan, S. Deep Hashing Network for Unsupervised Domain Adaptation, 2017.
- Volk, T., Ben-David, E., Amosy, O., Chechik, G., and Reichart, R. Example-based Hypernetworks for Out-of-Distribution Generalization, 2022.
- von Oswald, J., Henning, C., Grewe, B. F., and Sacramento, J. Continual learning with hypernetworks, 2022.
- Wang, H., He, Z., Lipton, Z. C., and Xing, E. P. Learning Robust Representations by Projecting Superficial Statistics Out, 2019.
- Wang, J., Liu, Q., Liang, H., Joshi, G., and Poor, H. V. Tackling the Objective Inconsistency Problem in Heterogeneous Federated Optimization, 2020.
- Wang, R., Huang, W., Shi, M., Wang, J., Shen, C., and Zhu, Z. Federated adversarial domain generalization network: A novel machinery fault diagnosis method with data privacy. *Knowledge-Based Systems*, 256:109880, 2022. ISSN 0950-7051.
- Yang, S., Choi, S., Park, H., Choi, S., Chang, S., and Yun, S. Client-agnostic Learning and Zero-shot Adaptation for Federated Domain Generalization, 2023.
- Yuan, J., Ma, X., Chen, D., Wu, F., Lin, L., and Kuang, K. Collaborative Semantic Aggregation and Calibration for Federated Domain Generalization, 2023.
- Zhang, L., Lei, X., Shi, Y., Huang, H., and Chen, C. Federated Learning with Domain Generalization, 2023a.
- Zhang, M. R., Lucas, J., Hinton, G., and Ba, J. Lookahead Optimizer: k steps forward, 1 step back, 2019.
- Zhang, R., Xu, Q., Yao, J., Zhang, Y., Tian, Q., and Wang, Y. Federated Domain Generalization With Generalization Adjustment. In *Proceedings of the IEEE/CVF Conference on Computer Vision and Pattern Recognition (CVPR)*, pp. 3954–3963, June 2023b.
- Zhang, W. and Li, X. Data privacy preserving federated transfer learning in machinery fault diagnostics using prior distributions. *Structural Health Monitoring*, 21(4): 1329–1344, 2022. doi: 10.1177/14759217211029201.
- Zhou, K., Liu, Z., Qiao, Y., Xiang, T., and Loy, C. C. Domain Generalization: A Survey. *IEEE Transactions on Pattern Analysis and Machine Intelligence*, pp. 1–20, 2022. doi: 10.1109/tpami.2022.3195549.

A. Appendix

A.1. Ablation Study

A.1.1. WORKINGS OF GRADALIGN

Figure 6 illustrates three aspects of the introduced gradient alignment technique. The bold line in the plot represents the maximum dissimilarity of a client’s gradient compared to the average client gradient, as expressed by the weight its gradient received in the hypernetwork update. Applying gradient alignment facilitates a directed global update and gradually diminishes the tendency to drift as the weights converge to a common value as training proceeds. For some left-out target domains, the proposed gradient alignment achieves near-optimal convergence, implying that no client is drifting further away from the average than another.

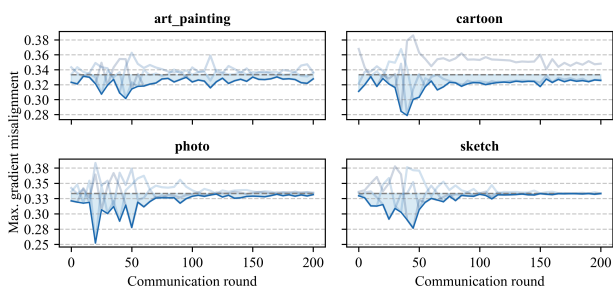


Figure 6. Convergence of gradient alignment weights. At each communication round, the aggregation weights based on the gradient alignment are depicted in transparent color per client. PACS; $d = 1$.

Additionally, to provide a comprehensive explanation of how GradAlign operates, we identify which clients exhibit significant weights in our experiments. The higher the weighting, the closer is the update direction proposed by the domain to the consensus direction. For certain data sets and combinations of source domains during training, we observe a higher tendency for domains to drift. For instance, ”photo” and ”sketch” of PACS reveal a higher disagreement on the common update direction than ”art_painting”. Conversely, ”photo” and ”sketch” drift less away from the consensus than ”cartoon” does, when seen during training. Compared to PACS, we identify larger drifts of certain domains on Office-Home and VLCS. Interestingly, every domain across all data sets assumes either a drift to or away from the consensus, depending on its combination with other source domains. This underscores the significant role of domain interactions in mastering a shared hypernetwork. Identifying easily interpretable similarities across domains proves challenging.

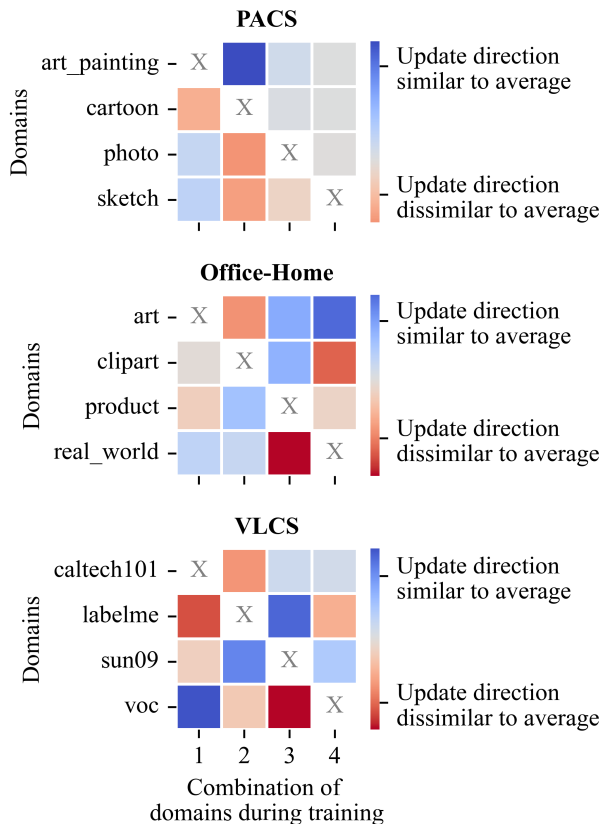


Figure 7. Final gradient alignment weights. At the end of the training (after 200 communication rounds), the aggregation weights of the gradient alignment are visualized. $d = 1$.

A.1.2. ADDED VALUE OF GRADALIGN AND EMA

Moreover, we investigate the introduced update rule of $hFedF$ in more detail. We conduct a direct comparison of GradAlign with simple averaging, and examine the impact of employing EMA versus its absence. Since both steps are not straightforward, Table 5 provides a rationale behind their introduction. The relative performance ($Acc_{hFedF} - Acc_{hFedF}^{(adapted)}$) of the different implementations among a data set are separately stated. Performance improvements of $hFedF$ with GradAlign and EMA compared to others are marked in green while performance losses are marked in red. The relative performance is averaged across all data splits (different d). On the PACS data set, the suggested $hFedF$ implementation (with GradAlign and EMA) outperforms all others wrt. *id*- and *ood*-accuracy, culminating at +1.3% and +1.7% performance gain respectively compared to the one without EMA. The value add of GradAlign and EMA is still apparent on Office-Home, where it improves on all alternatives.

Moreover, the performance gain of using GradAlign and EMA on PACS and Office-Home is more apparent in *ood*-

Table 5. Averaged accuracy across domains on all data sets without GradAlign and EMA.

DATA SET	ALGORITHM	$d = 1$		$d = 2$		$d = 3$		$\mu_{REL. PERFORMANCE}$	
		μ_{id}	μ_{ood}	μ_{id}	μ_{ood}	μ_{id}	μ_{ood}	μ_{id}	μ_{ood}
PACS	hFEDF	71.5	54.6	75.8	54.9	76.1	55.2		
	hFEDF (w/o GRADALIGN)	68.8	51.1	75.8	54.1	76.2	54.5	+0.9	+1.7
	hFEDF (w/o EMA)	70.7	53.4	76.0	55.2	76.5	54.5	+0.1	+0.5
	hFEDF (w/o GRADALIGN EMA)	68.5	50.8	75.3	54.7	75.8	54.2	+1.3	+1.7
OFFICE-HOME	hFEDF	49.4	29.8	52.1	31.2	52.2	31.7		
	hFEDF (w/o GRADALIGN)	49.2	30.2	51.9	31.2	51.5	31.4	+0.4	+0.0
	hFEDF (w/o EMA)	50.9	28.8	50.9	30.7	51.4	30.9	+0.2	+0.8
	hFEDF (w/o GRADALIGN EMA)	50.8	28.8	51.2	30.7	50.9	30.9	+0.3	+0.8
VLCS	hFEDF	66.1	56.9	66.8	58.1	65.7	58.7		
	hFEDF (w/o GRADALIGN)	66.0	58.8	67.0	58.6	66.3	58.4	-0.2	-0.7
	hFEDF (w/o EMA)	66.4	56.1	66.9	58.6	65.5	58.5	-0.1	-0.1
	hFEDF (w/o GRADALIGN EMA)	66.2	58.3	66.7	59.1	65.8	58.3	+0.0	-0.7

accuracy. As intended, this suggests that GradAlign and EMA encourage the hypernetwork to generate a highly-generalizable model.

However, the implementation of *hFedF* introduced in Algorithm 1 is not able to match the performances of the ones without GradAlign and EMA on the VLCS data set. The VLCS data set is the only data set containing purely photo-realistic domains. Notably, VLCS is considered to offer the most challenging classification task among the ones in this paper³. The difficulty of VLCS lies predominantly in the representation of the images. The objects to be classified are often unobtrusively illustrated and their features are less dominant depicted than in other data sets. The domains of VLCS are merely defined by different data sets of photos whose resolution, color correctness, lighting, depiction of objects and general appearance differ from each other. It might be that the gradient alignment technique and subsequently the hypernetwork struggle to find common data representation across all domains of VLCS. In consequence, after each local update the clients (domains) propose very unaligned update directions for the hypernetwork, compromising its convergence. Thus the challenge of VLCS might be highly domain-based, which could call into question the effectiveness of GradAlign and EMA - both are initially designed to stabilize the update of the hypernetwork in the short term. This reasoning is also supported by the fact that the GradAlign weights of VLCS exhibit the highest discrepancy at the end of the training, shown already in Figure 7.

³First, the results of hFedF and other benchmarks exhibit low accuracies on VLCS, compared to PACS and Office-Home, considering the number of classes. Second, even state-of-the-art benchmark algorithms for non-federated DG demonstrate performance issues on VLCS, compared to PACS and Office-Home (Paper-[sWithCode](#), c;a;b).

A.1.3. PRE-LEARNED CLIENT EMBEDDINGS

For the reported results in the main body, the client embeddings are learnable with a dimension of 1. We use an Autoencoder to obtain a data-conditioned, fixed (“non-learnable”) embeddings. Its architecture is depicted in Figure 9. Prior to federated training, each client receives the same Autoencoder and trains it locally on 100 training images. The Autoencoder compresses the images and finds a latent data representation. The final embedding is obtained by taking the mean of the latent vectors of all validation images. In this way, each client transmits an embedding to the server, describing its local data distribution. Figure 8 shows that neither the embedding dimension nor the learnability can improve the performance majorly.

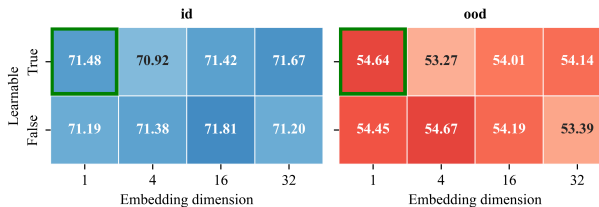


Figure 8. Variations of client embeddings. PACS; $d = 1$.

A.1.4. IMPORTANCE OF CLIENT EMBEDDING

To provide a clear and well-supported explanation of the role of client embedding, we further investigate the significance of the client embeddings based on empirical evidence. In particular, we scrutinize the general implication of learning client embeddings in the proposed setting based on two lessons learned. 1) The observations in Figure 8 conclude that the learnability and dimension of the client embeddings have minor impact on the general performance, and 2) Figure 4 indicates that the hypernetwork prioritizes the over-

Table 6. Averaged accuracy across domains on all data sets for randomized client embeddings.

DATA SET	ALGORITHM	$d = 1$		$d = 2$		$d = 3$	
		μ_{id}	μ_{ood}	μ_{id}	μ_{ood}	μ_{id}	μ_{ood}
PACS	hFEDF	71.5	54.6	75.8	54.9	76.1	55.2
	hFEDF (RAND. EMBED.)	71.1	53.9	75.1	54.8	75.7	54.5
OFFICE-HOME	hFEDF	49.4	29.8	52.1	31.2	52.2	31.7
	hFEDF (RAND. EMBED.)	48.2	31.0	51.0	31.8	51.8	30.9
VLCS	hFEDF	66.1	56.9	66.8	58.1	65.7	58.7
	hFEDF (RAND. EMBED.)	65.8	55.7	66.7	58.1	65.7	58.4

all data distribution over the specific distributions within individual clients. This is evident as the disparities in distribution between clients are not captured in the learned client embeddings.

To retrieve further insights, we randomize (reinitialize) the client embeddings after every server update and compare the results to the original implementation in Table 6. Within each data set the better accuracy is marked in **bold**. Although *hFedF* with learned client embeddings surpasses the version with randomized client embeddings, the results remain remarkably consistent. On the one hand, this impressive finding advocates that the hypernetwork inherently simply acts a non-linear fusion of NNs, effectively disregarding the data distribution of the clients. On the other hand, this observation argues for higher data privacy standards since the client embeddings do not hold any reliable information, which could be misappropriated. In fact, as observed in Table 6, they can even be randomized in the process of the federated training and still perform adequately.

A.1.5. ADDING CLIENTS

For the following experiments *FedAvg* and *FedSR* are selected as comparing algorithms since they consistently show the most consistent performance for general *non-iid* data and FDG, respectively. The following results showcase the robustness of the proposed algorithm.

For any FL algorithm, the ability to absorb an expanding number of clients without dramatic performance degradation is as important as retaining the performance over time. Figure 9 unveils how the proposed methods remain sovereign in both *id*- and *ood*-accuracy for an increasing number of clients.

A.1.6. CHOOSING THE NUMBER OF LOCAL EPOCHS

Figure 10 compares different numbers of local epochs. With an increasing number of epochs, the convergence speed increases. All algorithms show a comparable tendency towards the number of local epochs. To tradeoff convergence speed and computational costs, the number of local epochs

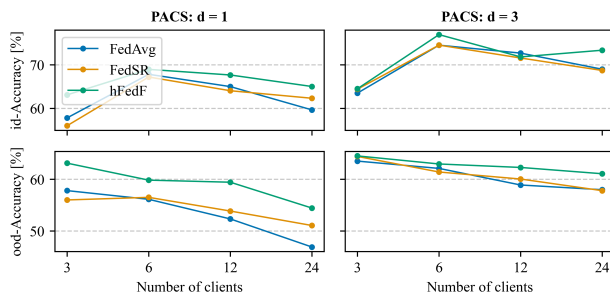


Figure 9. Expanded number of clients. PACS ("photo"); $d = 1$.

is fixed for all experiments to 2.

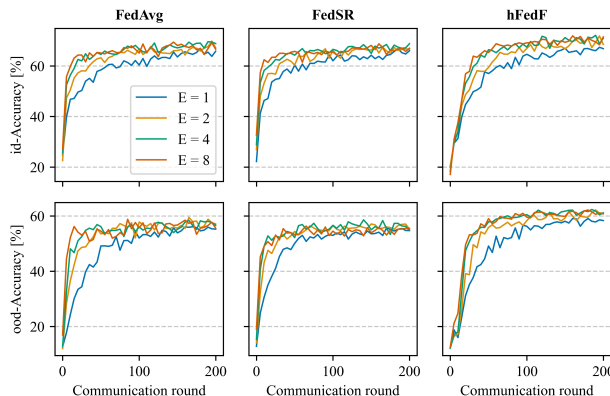


Figure 10. Impact of the number of local epochs on the convergence speed. PACS ("photo"); $d = 1$

A.1.7. LONG-TERM BEHAVIOR

The proposed algorithm maintains the personalization and generalization performance over many communication rounds. Preventing performance degradation over time is an important property of an FL algorithm because they are mostly applied in scenarios where life-long learning is expected. Figure 11 shows that the proposed algorithm does not lose performance as the number of communication

rounds increases.

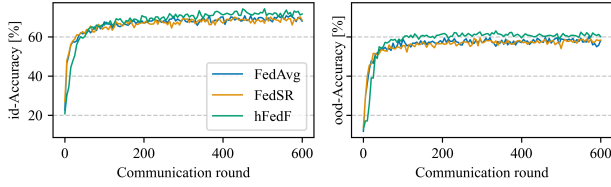


Figure 11. Expanded number of communication rounds. PACS ("photo"); $d = 1$.

A.1.8. IMPACT OF EMA REGULARIZATION

In Figure 12, the effect of different values of α for EMA are visualized. As expected, the lower α , the more regularized the hypernetwork updates, resulting in flatter but less fluctuating convergence curves. To benefit from a desirable tradeoff, α is chosen between 0.75 and 0.95.

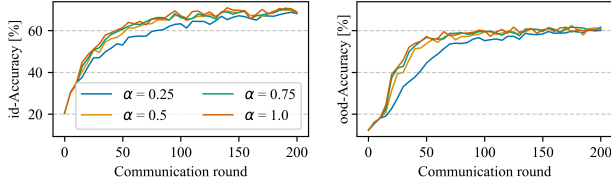


Figure 12. Influence of the weight decay of EMA. PACS ("photo"); $d = 1$.

A.1.9. FROM ZERO- TO FEW-SHOT LEARNING

Additionally, the performance is evaluated on a relaxation of the DG problem by adding a few-shots of the target domain to each client during training. As expected, the performance gain on generalization dominates with an increasing number of shots - shown in Figure 13. Each client obtains knowledge about the *ood*-domain, which makes prediction on that specific domain easier. At the same time, the data on each client gets more diverse, which makes *id*-prediction more challenging. The proposed algorithm is mostly able to maintain its superiority compared to the other benchmarks.

A.2. Experimental Details

A.2.1. ALGORITHMS

The algorithm of our proposed strategy is presented that allocates the source domains to the clients and thereby manages the severeness of domain shift across the clients. In detail, the minimum number of partitions a required for each domain is first calculated. Additionally, the number of domains b that need to be split into one extra partition is determined. This is necessary because it is not guaranteed that all domains can be split by the same number to

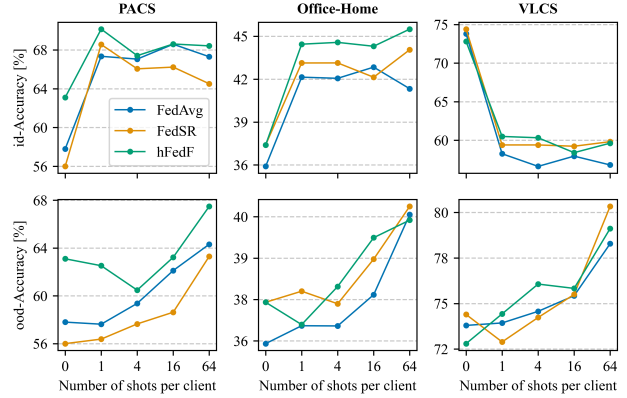


Figure 13. Few-shot learning. PACS ("photo"); $d = 1$.

satisfy the constraint of having precisely d domains on each client. Subsequently, the domains are split evenly, with the b largest domains being divided into one extra partition if necessary. Next, the partitions of the respective domains are randomly distributed among the clients while adhering to the constraint d .

Algorithm 2 Client Update (ClientUpdate)

Require: μ - learning rate of client, \mathcal{D} - data of client, $f(\cdot; \tilde{\varphi})$ - client model
for $x, y \in \mathcal{D}$ **do**
 $\hat{y} \leftarrow f_c(x; \tilde{\varphi})$
 $\mathcal{L} \leftarrow \ell_{\text{cross-entropy}}(y, \hat{y})$
 $\tilde{\varphi} \leftarrow \tilde{\varphi} - \mu \cdot \nabla_{\varphi} \mathcal{L}$
end for
Return i : $\tilde{\varphi}$

Algorithm 3 Gradient Alignment (GradAlign)

Require: \mathcal{S} - set of clients, g_i - local gradient of client i
 compute $g_{\text{avg}} \leftarrow \frac{1}{|\mathcal{S}|} \sum_{i \in \mathcal{S}} g_i$
for client $i \in \mathcal{S}$ **do**
 $\gamma_i^t \leftarrow \cos(g_{\text{avg}}, g_i)$
 $\tilde{\gamma}_i \leftarrow \text{softmax}(\gamma_i)$
end for
Return (client i): $\tilde{\gamma}_i$

For the sake of completeness and reproducibility, the supplementary algorithms to Algorithm 1 are provided.

A.2.2. SELECTED MODELS

The architectures of the hypernetwork (Figure 8) and the client model (Figure 7) are optimized regarding the number of layers, the number of hidden units, the application of activation functions, and the configuration of the convolutional layers. The hypernetwork uses *LeakyReLU* activation functions to propagate the gradients more effectively and

Algorithm 4 Exponential Moving Average (EMA)

Require: θ^t - parameters of hypernetwork, t - communication round, $w \in \mathbb{Z}^+$ - warm-up round, $\alpha \in [0, 1]$ - smoothing factor

if warm-up round is reached ($t = w$) **then**

Initialize: $\theta_{\text{EMA}}^t \leftarrow \theta^t$

end if

if $t > w$ **then**

$\theta_{\text{EMA}}^{t+1} \leftarrow \alpha\theta^t + (1 - \alpha)\theta_{\text{EMA}}^t$

$\theta^t \leftarrow \theta_{\text{EMA}}^{t+1}$

end if

Return: θ^t

an Adam optimizer for improved numerical stability during training (Chauhan et al., 2023). Furthermore, the last layer of the Autoencoder is activated with a *Sigmoid* function to ensure valid pixel values. Note that the number of clients and the embedding dimension are N and e respectively.

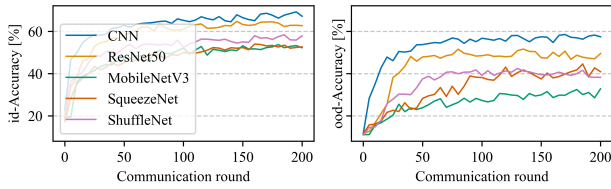


Figure 14. Evaluation of FedAvg on different state-of-the-art architectures as client models. *PACS* ("photo"); $d = 1$.

Choosing a hypernetwork approach in FL imposes constraints on the model architecture of the client. The complexity of the client model directly impacts the memory demands of the hypernetwork and can hinder its convergence stability. Therefore, we tried to find a high-performing client model architecture while avoiding undesirable computational complexities and excessive memory consumption. Throughout this research, targeted exploration of neural architectures was conducted to minimize the parameter count while maximizing the predictive performance. The resulting architecture is a Convolutional NN inspired by the *Inception* architecture (Szegedy et al., 2014). *Inception* remains one of the most successful neural networks for image classification and stands out with its simple modularization and computational efficiency. To approve the design of the client model architecture, the performance of FedAvg compared to well-established networks is rolled out in Figure 14.

A.2.3. HYPERPARAMETER SEARCH

Table 10 depicts the search grid and the selected values for each hyperparameter, which was tuned to benchmark the algorithm. Thereby, the goal is to maintain fairness in the tuning process without overextending computational

Algorithm 5 Data split

Require: $N > 1$ - number of clients, d - number of source domains per client, $\{\mathcal{D}_j\}_{j \in \mathcal{Z}_{\text{src}}}$ - data sets of source domains

$a \leftarrow \lfloor \frac{N \cdot d}{|\mathcal{Z}_{\text{src}}|} \rfloor$

$b \leftarrow \text{mod}(N \cdot d, |\mathcal{Z}_{\text{src}}|)$

for each \mathcal{D}_j **do**

if \mathcal{D}_j is part of b largest data sets **then**

$\text{SplitRule} \leftarrow [\frac{1}{a+1}, \dots, \frac{1}{a+1}]^{a+1}$

else

$\text{SplitRule} \leftarrow [\frac{1}{a}, \dots, \frac{1}{a}]^a$

end if

split \mathcal{D}_j randomly according to SplitRule

$\text{subsets}_j \leftarrow \text{split } \mathcal{D}_j$

end for

for 1 to d do

for client $i \in \{1, \dots, N\}$ **do**

for domain $j \in \mathcal{Z}_{\text{src}}$ **do**

if subsets_j has splits **then**

append first element of subsets_j to subsets_i

remove first element of subsets_j

break out of inner loop

end if

end for

end for

for client $i \in \{1, \dots, N\}$ **do**

concatenate elements in subsets_i

$\mathcal{D}_i \leftarrow \text{concatenated subsets}_i$

end for

Return (client i): \mathcal{D}_i

resources. For the non-federated methods, namely *Central* and *Local*, the hyperparameters of FedAvg are adopted. A consistent search grid was chosen across all data sets and algorithms, where the reference values are determined either by consulting the original papers of the respective algorithms or by adhering to the benchmarking suggestions for FDG (Bai et al., 2023). The final value is chosen based on the optimal performance observed in a single run with a specific seed for a designated target domain after 100 communication rounds.

Table 7. Detailed architecture of the client model.

LAYER	OUTPUT SHAPE	CONFIGURATION	ACTIVATION
CONVOLUTIONAL	[-1, 32, 32, 32]	K = 3; S = 1; P = 1	-
MAXPOOL	[-1, 32, 16, 16]	K = 2; S = 2; P = 0	RELU
CONVOLUTIONAL	[-1, 32, 16, 16]	K = 1; S = 1; P = 0	-
CONVOLUTIONAL	[-1, 64, 16, 16]	K = 3; S = 1; P = 1	-
MAXPOOL	[-1, 64, 8, 8]	K = 2; S = 2; P = 0	RELU
INCEPTION MODULE	[-1, 176, 8, 8]	INT. CHANNELS = [32, 64, 16]	RELU
INCEPTION MODULE	[-1, 288, 8, 8]	INT. CHANNELS = [32, 64, 16]	RELU
ADAPTIVEAVGPOOL	[-1, 288, 3, 3]	OUTPUT SIZE = 3	-
FLATTEN	[-1, 2592]	-	-
DROPOUT	[-1, 2592]	RATIO = 0.2	-
LINEAR	[-1, 256]	-	-
LINEAR	[-1, n_{CLASSES}]	-	-

ABBREVIATIONS: K - KERNEL SIZE; S - STRIDE; P - PADDING; INT. - INTERMEDIATE.

Table 8. Detailed architecture of the hypernetwork.

LAYER	OUTPUT SHAPE	ACTIVATION
EMBEDDING ^A	[1, e]	-
LINEAR ^B	[1, 50]	LEAKYRELU
LINEAR ^B	[1, 50]	LEAKYRELU
LINEAR ^B	[1, 50]	LEAKYRELU
LINEAR ^B	[1, 50]	-
MULTI-HEAD LINEAR ^B	[1, n_{LAYERS} , $n_{\text{PARAMETERS OF LAYER}}$]	-

^A THE PARAMETERS OF THIS LAYER ARE DEFINED BY ν OF EQUATION 4. THE EMBEDDING LAYER ν HAS A SHAPE OF $[N, e]$. THE HYPERNETWORK TAKES THE CLIENT ID AS AN INDEX AND USES IT TO RETRIEVE THE CORRESPONDING EMBEDDING FROM THE EMBEDDING LAYER.

^B THE PARAMETERS OF THESE LAYERS ARE DEFINED BY θ OF EQUATION 4.

Table 9. Detailed architecture of the Autoencoder.

LAYER	OUTPUT SHAPE	CONFIGURATION	ACTIVATION
CONV	[-1, 16, 32, 32]	K = 3; S = 1; P = 1	RELU
MAXPOOL	[-1, 16, 16, 16]	K = 2; S = 2; P = 0	-
CONV	[-1, 32, 16, 16]	K = 3; S = 1; P = 1	RELU
MAXPOOL	[-1, 32, 8, 8]	K = 2; S = 2; P = 0	-
FLATTEN	[-1, 2048]	-	-
LINEAR	[-1, e]	-	-
LINEAR	[-1, 2048]	-	-
CONVTRANSPOSE	[-1, 16, 16, 16]	K = 2; S = 2; P = 0	RELU
CONVTRANSPOSE	[-1, 3, 32, 32]	K = 2; S = 2; P = 0	SIGMOID

ABBREVIATIONS: CONV - CONVOLUTIONAL; K - KERNEL SIZE; S - STRIDE; P - PADDING.

Table 10. Detailed search grid and selected values of hyperparameters for all algorithms and data sets.

ALGORITHM	HYPERPARAMETER	GRID	SELECTED VALUE		
			PACS	OFFICE-HOME	VLCS
FEDAVG	CLIENT LEARNING RATE	{1E-3, 1E-4, 1E-5}	1E-3	1E-3	1E-4
	CLIENT WEIGHT DECAY	{1E-3, 1E-4, 1E-5}	1E-4	1E-5	1E-4
FEDPROX	CLIENT LEARNING RATE	{1E-3, 1E-4, 1E-5}	1E-3	1E-3	1E-3
	CLIENT WEIGHT DECAY	{1E-3, 1E-4, 1E-5}	1E-4	1E-4	1E-4
	L_2 REGULARIZER	{1E-1, 1E-2, 1E-3}	1E-2	1E-2	1E-2
pFEDHN	SERVER LEARNING RATE	{1E-1, 1E-2, 1E-3}	1E-2	1E-3	1E-3
	SERVER WEIGHT DECAY	{1E-3, 1E-4, 1E-5}	1E-3	1E-4	1E-4
	CLIENT LEARNING RATE	{1E-3, 1E-4, 1E-5}	1E-3	1E-3	1E-3
	CLIENT WEIGHT DECAY	{1E-3, 1E-4, 1E-5}	1E-5	1E-4	1E-4
FEDSR	CLIENT LEARNING RATE	{1E-3, 1E-4, 1E-5}	1E-3	1E-3	1E-3
	CLIENT WEIGHT DECAY	{1E-3, 1E-4, 1E-5}	1E-5	1E-4	1E-4
	L_2 REGULARIZER	{1E-1, 1E-2, 1E-3}	1E-1	1E-1	1E-2
FEDGMA	CLIENT LEARNING RATE	{1E-3, 1E-4, 1E-5}	1E-3	1E-3	1E-3
	CLIENT WEIGHT DECAY	{1E-3, 1E-4, 1E-5}	1E-4	1E-4	1E-4
	MASK THRESHOLD	{0.3, 0.5, 0.7}	0.7	0.3	0.5
	SERVER STEP SIZE	{1E-0, 1E-1, 1E-2}	1E-0	1E-2	1E-2
hFEDF	SERVER LEARNING RATE	{1E-1, 1E-2, 1E-3}	1E-3	1E-3	1E-3
	SERVER WEIGHT DECAY	{1E-3, 1E-4, 1E-5}	1E-5	1E-5	1E-3
	SERVER EMA DECAY	{0.75, 0.85, 0.95}	0.95	0.75	0.75
	CLIENT LEARNING RATE	{1E-3, 1E-4, 1E-5}	1E-3	1E-3	1E-3
	CLIENT WEIGHT DECAY	{1E-3, 1E-4, 1E-5}	1E-3	1E-3	1E-3

A.3. Detailed Results

The detailed results are derived from the final evaluation after 200 communication rounds, averaged across three seeds - including the standard deviation. The *id*- and *ood*-accuracy are separately stated for each left-out target domain. Each data set has in total 4 domains, where 3 are seen overall during training, and 1 is left-out for *ood*-testing. The averages across all combinations of source and target domain are marked in **bold** and correspond to the same numbers reported in Subsection 4.2. Since the centralized method holds in every case 3 source domains, its performances are only presented for $d = 3$. The training curves are averaged across target domains and seeds, and are measured every 5 communication rounds. All computations are conducted on two NVIDIA RTX A5000 24GB GPUs.

A.3.1. PACS

Table 11. Accuracy evaluated on PACS; $d = 1$.

	<i>Acc_{id}</i>					<i>Acc_{ood}</i>				
	A	C	P	S	μ	A	C	P	S	μ
CENTRAL	-	-	-	-	-	-	-	-	-	-
LOCAL	82.3 ± 3.6	74.9 ± 12.6	74.4 ± 12.1	73.8 ± 9.7	76.4	28.4 ± 8.0	34.3 ± 6.5	41.9 ± 18.5	38.8 ± 6.4	35.8
FEDAVG	73.4 ± 9.5	69.8 ± 15.3	67.3 ± 12.8	70.0 ± 6.1	70.1	37.8 ± 1.1	50.4 ± 0.6	57.8 ± 1.0	59.2 ± 1.5	51.3
FEDPROX	73.8 ± 8.8	70.0 ± 13.6	67.2 ± 14.0	68.7 ± 8.2	69.9	36.1 ± 1.7	51.7 ± 1.8	56.1 ± 0.5	58.7 ± 1.3	50.7
PFEDHN	69.8 ± 9.9	65.2 ± 14.1	60.3 ± 11.1	65.4 ± 10.8	65.2	36.0 ± 6.9	47.1 ± 4.1	55.7 ± 6.1	54.2 ± 1.3	48.2
FEDSR	73.0 ± 9.3	67.5 ± 14.2	67.3 ± 13.7	68.9 ± 9.4	69.2	35.8 ± 0.7	47.7 ± 2.3	56.0 ± 1.0	55.8 ± 0.8	48.9
FEDGMA	73.6 ± 8.4	67.8 ± 14.0	65.3 ± 14.5	67.9 ± 9.1	68.7	37.4 ± 1.0	49.8 ± 2.3	56.3 ± 2.0	54.8 ± 1.0	49.6
hFEDF	75.4 ± 6.1	70.6 ± 14.0	70.9 ± 7.5	69.1 ± 10.6	71.5	42.4 ± 0.3	51.9 ± 0.3	63.1 ± 1.3	61.2 ± 0.9	54.6

ABBREVIATIONS: μ - AVERAGE; A - ART PAINTING; C - CARTOON; P - PHOTO; S - SKETCH.

Table 12. Accuracy evaluated on PACS; $d = 2$.

	<i>Acc_{id}</i>					<i>Acc_{ood}</i>				
	A	C	P	S	μ	A	C	P	S	μ
CENTRAL	-	-	-	-	-	-	-	-	-	-
LOCAL	78.1 ± 3.3	69.8 ± 7.7	72.5 ± 6.0	65.5 ± 7.5	71.5	34.0 ± 2.1	42.4 ± 3.8	52.7 ± 7.5	44.2 ± 3.8	43.3
FEDAVG	80.9 ± 1.1	74.0 ± 8.4	75.5 ± 6.7	71.7 ± 5.8	75.5	42.3 ± 1.0	51.5 ± 0.3	62.8 ± 1.2	56.0 ± 1.4	53.2
FEDPROX	80.6 ± 3.7	73.7 ± 7.8	75.7 ± 6.3	70.3 ± 5.3	75.1	41.4 ± 0.8	52.8 ± 1.2	62.9 ± 1.0	54.9 ± 0.3	53.0
PFEDHN	77.7 ± 4.8	71.6 ± 5.8	73.9 ± 5.0	65.4 ± 7.0	72.2	40.6 ± 0.6	50.8 ± 1.5	58.3 ± 2.4	52.5 ± 5.1	50.6
FEDSR	79.2 ± 2.7	72.4 ± 8.2	74.3 ± 8.1	69.4 ± 4.1	73.8	40.9 ± 0.5	50.2 ± 2.7	61.9 ± 1.2	53.5 ± 2.7	51.6
FEDGMA	74.6 ± 4.8	69.7 ± 7.4	71.1 ± 7.3	67.1 ± 6.4	70.6	38.6 ± 1.4	48.6 ± 0.7	60.1 ± 2.1	52.5 ± 3.1	49.9
hFEDF	78.2 ± 2.5	74.9 ± 5.8	76.3 ± 5.2	73.9 ± 4.5	75.8	44.1 ± 0.7	54.4 ± 0.8	62.3 ± 1.5	58.7 ± 0.4	54.9

ABBREVIATIONS: μ - AVERAGE; A - ART PAINTING; C - CARTOON; P - PHOTO; S - SKETCH.

Table 13. Accuracy evaluated on PACS; $d = 3$.

	<i>Acc_{id}</i>					<i>Acc_{ood}</i>				
	A	C	P	S	μ	A	C	P	S	μ
CENTRAL	80.4 ± 1.5	75.5 ± 0.9	74.9 ± 1.5	70.7 ± 1.1	75.4	40.8 ± 1.2	53.1 ± 1.1	65.0 ± 0.7	55.8 ± 0.5	53.7
LOCAL	75.1 ± 2.6	71.0 ± 2.8	69.3 ± 1.7	62.9 ± 4.8	69.6	35.2 ± 1.9	46.6 ± 3.1	55.2 ± 4.4	46.7 ± 4.5	45.9
FEDAVG	81.8 ± 2.2	76.2 ± 1.9	78.1 ± 2.1	71.6 ± 2.7	76.9	40.7 ± 0.5	54.1 ± 1.2	63.5 ± 0.5	55.6 ± 1.9	53.5
FEDPROX	81.0 ± 3.3	78.2 ± 1.0	76.9 ± 2.3	73.1 ± 3.3	77.3	41.1 ± 0.7	54.6 ± 1.2	63.0 ± 0.7	56.3 ± 0.9	53.8
PFEDHN	78.4 ± 2.2	76.0 ± 2.8	72.8 ± 1.3	70.1 ± 3.4	74.3	38.4 ± 0.7	55.0 ± 0.5	60.8 ± 1.7	50.0 ± 2.7	51.1
FEDSR	80.4 ± 1.9	75.2 ± 3.0	75.8 ± 2.1	71.8 ± 4.5	75.8	38.9 ± 1.0	52.4 ± 0.8	64.4 ± 0.9	53.2 ± 0.3	52.2
FEDGMA	78.2 ± 3.0	74.2 ± 2.5	72.0 ± 4.5	66.6 ± 3.6	72.7	38.5 ± 0.8	50.8 ± 1.6	60.7 ± 1.9	49.6 ± 3.6	49.9
hFEDF	80.8 ± 3.8	75.9 ± 2.7	75.2 ± 2.1	72.3 ± 3.5	76.1	42.8 ± 0.5	55.6 ± 0.8	64.5 ± 0.9	57.9 ± 1.1	55.2

ABBREVIATIONS: μ - AVERAGE; A - ART PAINTING; C - CARTOON; P - PHOTO; S - SKETCH.

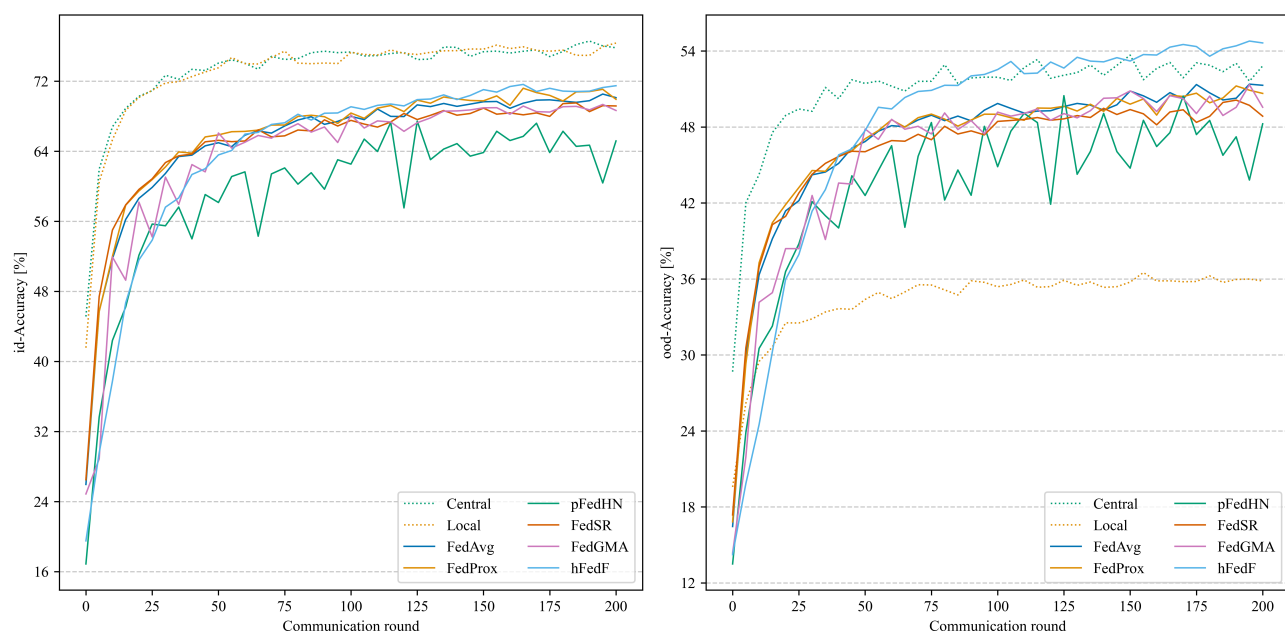


Figure 15. Evaluation curves. PACS; $d = 1$.

A.3.2. OFFICE-HOME

Table 14. Accuracy evaluated on Office-Home; $d = 1$.

	Acc_{id}					Acc_{ood}				
	A	C	P	R	μ	A	C	P	R	μ
CENTRAL	-	-	-	-	-	-	-	-	-	-
LOCAL	55.1 ± 10.8	44.8 ± 15.1	40.4 ± 15.1	50.5 ± 17.7	47.7	11.8 ± 4.0	16.5 ± 4.5	20.8 ± 8.8	19.6 ± 2.3	17.2
FEDAVG	54.3 ± 7.4	46.1 ± 15.2	43.2 ± 12.2	47.6 ± 19.3	47.8	19.3 ± 0.5	26.5 ± 1.1	35.9 ± 0.5	34.5 ± 0.5	29.1
FEDPROX	54.7 ± 8.0	46.6 ± 15.2	44.8 ± 10.8	48.2 ± 18.4	48.6	19.3 ± 0.5	26.4 ± 0.6	36.6 ± 0.4	34.1 ± 0.8	29.1
PFEDHN	57.1 ± 11.0	48.8 ± 16.0	43.9 ± 13.3	49.7 ± 16.6	49.9	13.9 ± 4.2	20.3 ± 4.3	26.2 ± 8.4	24.1 ± 3.5	21.1
FEDSR	54.5 ± 7.2	46.5 ± 14.9	44.3 ± 12.5	46.8 ± 18.0	48.1	19.3 ± 0.8	27.6 ± 0.9	37.4 ± 0.9	34.3 ± 0.7	29.6
FEDGMA	54.4 ± 7.4	45.7 ± 14.4	43.1 ± 11.7	47.7 ± 18.8	47.7	19.5 ± 0.5	26.4 ± 1.0	37.3 ± 0.4	34.6 ± 0.5	29.5
hFEDF	56.8 ± 8.2	47.1 ± 12.6	44.2 ± 10.8	49.6 ± 16.6	49.4	20.0 ± 0.8	28.4 ± 0.6	37.4 ± 1.3	33.4 ± 3.2	29.8

ABBREVIATIONS: μ - AVERAGE; A - ART; C - CLIPART; P - PRODUCT; R - REAL WORLD.

Table 15. Accuracy evaluated on Office-Home; $d = 2$.

	Acc_{id}					Acc_{ood}				
	A	C	P	R	μ	A	C	P	R	μ
CENTRAL	-	-	-	-	-	-	-	-	-	-
LOCAL	45.6 ± 4.7	38.4 ± 8.2	34.7 ± 5.5	43.4 ± 5.1	40.5	13.7 ± 2.7	18.3 ± 1.6	23.7 ± 4.9	23.2 ± 2.3	19.7
FEDAVG	57.2 ± 4.4	50.3 ± 6.5	44.5 ± 5.7	53.3 ± 4.6	51.3	19.2 ± 0.6	26.7 ± 0.5	37.0 ± 1.0	34.9 ± 0.6	29.4
FEDPROX	56.8 ± 3.6	49.6 ± 7.7	45.2 ± 5.8	54.4 ± 3.8	51.5	19.9 ± 0.7	26.8 ± 0.3	37.0 ± 0.8	35.2 ± 0.5	29.7
PFEDHN	50.2 ± 4.7	43.2 ± 7.9	40.1 ± 5.4	46.7 ± 8.7	45.1	16.0 ± 1.7	21.7 ± 2.7	28.9 ± 4.1	27.7 ± 4.4	23.6
FEDSR	56.9 ± 4.0	50.0 ± 7.0	46.4 ± 5.1	52.7 ± 5.1	51.5	19.8 ± 0.3	26.6 ± 0.3	36.9 ± 1.1	35.7 ± 0.6	29.8
FEDGMA	57.4 ± 3.3	50.1 ± 6.8	44.6 ± 5.0	53.4 ± 4.3	51.4	20.1 ± 0.0	27.4 ± 0.3	37.2 ± 0.6	35.4 ± 0.3	30.0
hFEDF	56.4 ± 4.0	52.1 ± 6.6	46.1 ± 4.3	54.0 ± 5.6	52.1	20.4 ± 1.0	28.5 ± 1.1	38.8 ± 0.6	37.2 ± 0.6	31.2

ABBREVIATIONS: μ - AVERAGE; A - ART; C - CLIPART; P - PRODUCT; R - REAL WORLD.

Table 16. Accuracy evaluated on Office-Home; $d = 3$.

	Acc_{id}					Acc_{ood}				
	A	C	P	R	μ	A	C	P	R	μ
CENTRAL	54.1 ± 0.6	47.4 ± 1.4	44.4 ± 0.7	52.1 ± 1.5	49.5	18.5 ± 1.1	25.7 ± 0.6	35.7 ± 0.3	32.5 ± 1.1	28.1
LOCAL	40.4 ± 1.9	36.4 ± 3.4	32.8 ± 2.1	38.0 ± 2.4	36.9	13.9 ± 0.8	19.0 ± 0.8	25.5 ± 0.8	24.9 ± 1.0	20.8
FEDAVG	56.1 ± 3.1	50.5 ± 1.5	45.9 ± 3.8	54.4 ± 3.5	51.7	19.5 ± 0.4	26.4 ± 0.5	36.9 ± 0.4	34.8 ± 0.5	29.4
FEDPROX	56.1 ± 2.7	49.3 ± 2.2	46.0 ± 3.6	56.0 ± 3.1	51.8	19.6 ± 0.2	26.2 ± 0.2	38.0 ± 0.6	35.7 ± 0.3	29.9
PFEDHN	48.8 ± 2.3	40.5 ± 6.5	40.1 ± 3.5	46.6 ± 4.2	44.0	17.2 ± 1.0	22.5 ± 3.5	32.4 ± 2.1	31.1 ± 2.5	25.8
FEDSR	56.3 ± 2.3	50.6 ± 1.7	46.3 ± 2.7	54.7 ± 2.2	52.0	19.7 ± 1.3	26.6 ± 0.8	37.9 ± 0.6	36.4 ± 0.7	30.2
FEDGMA	56.2 ± 2.2	49.1 ± 2.1	46.3 ± 3.4	55.4 ± 3.9	51.7	20.3 ± 0.3	26.3 ± 0.3	36.8 ± 0.7	35.0 ± 1.0	29.6
hFEDF	56.6 ± 2.3	50.3 ± 1.7	47.4 ± 3.8	54.4 ± 2.9	52.2	20.9 ± 0.5	29.0 ± 0.8	39.5 ± 0.3	37.4 ± 0.6	31.7

ABBREVIATIONS: μ - AVERAGE; A - ART; C - CLIPART; P - PRODUCT; R - REAL WORLD.

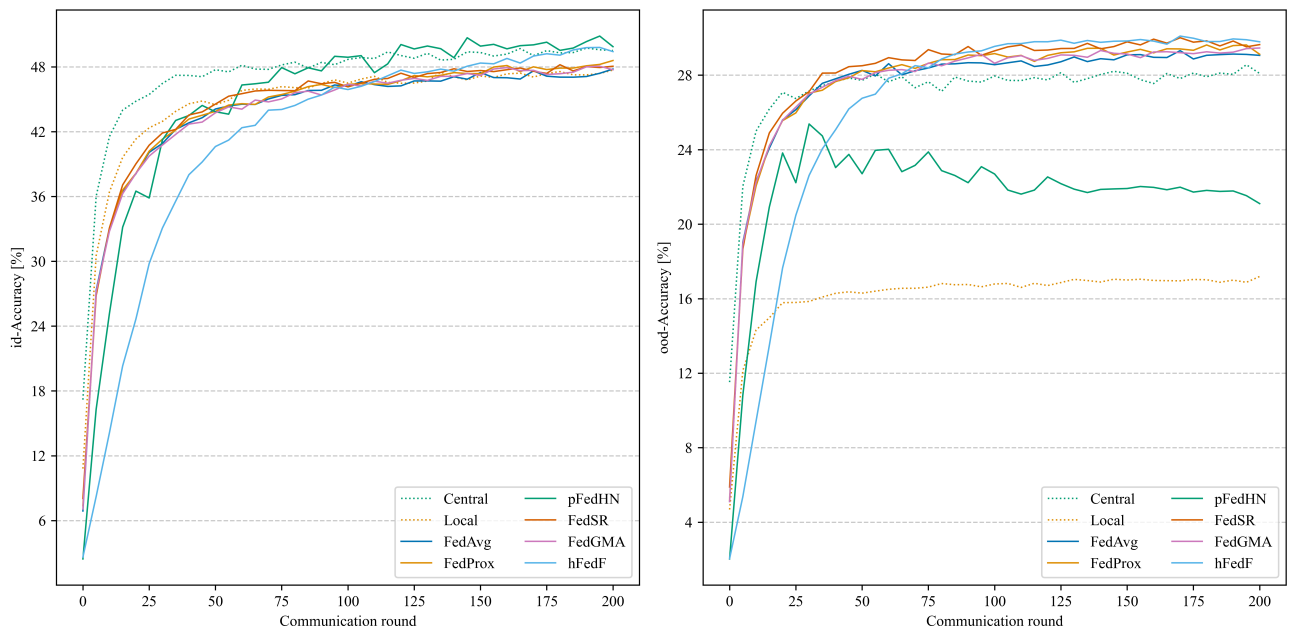


Figure 16. Evaluation curves. *Office-Home*; $d = 1$.

A.3.3. VLCS

Table 17. Accuracy evaluated on VLCS; $d = 1$.

	Acc_{id}					Acc_{ood}				
	C	L	S	V	μ	C	L	S	V	μ
CENTRAL	-	-	-	-	-	-	-	-	-	-
LOCAL	62.4 ± 3.0	71.6 ± 17.4	70.5 ± 17.3	75.1 ± 15.4	69.9	60.4 ± 12.4	41.5 ± 14.5	36.5 ± 12.5	36.2 ± 10.3	43.6
FEDAVG	57.8 ± 4.1	67.6 ± 10.6	70.3 ± 14.8	66.7 ± 10.4	65.6	73.8 ± 1.6	54.8 ± 0.5	54.5 ± 1.3	48.7 ± 1.7	58.0
FEDPROX	56.3 ± 3.8	67.5 ± 13.4	68.6 ± 15.5	69.2 ± 10.8	65.4	73.0 ± 1.9	53.3 ± 0.8	51.7 ± 0.7	46.8 ± 0.8	56.2
PFEDHN	58.2 ± 8.7	65.1 ± 20.2	63.3 ± 23.9	67.2 ± 19.3	63.4	70.0 ± 5.4	48.0 ± 8.0	41.9 ± 8.5	40.2 ± 6.9	50.0
FEDSR	59.9 ± 3.8	65.9 ± 12.5	69.8 ± 15.0	68.2 ± 11.4	66.0	74.4 ± 0.5	54.4 ± 0.5	51.1 ± 1.1	49.2 ± 0.4	57.2
FEDGMA	59.4 ± 4.0	68.0 ± 13.4	69.0 ± 16.2	69.3 ± 10.1	66.4	73.6 ± 1.6	55.0 ± 0.8	51.8 ± 1.6	47.5 ± 0.6	57.0
hFEDF	58.4 ± 3.3	68.4 ± 16.8	68.2 ± 16.6	69.4 ± 13.8	66.1	72.8 ± 0.7	52.6 ± 2.4	53.9 ± 0.3	48.4 ± 1.7	56.9

ABBREVIATIONS: μ - AVERAGE; C - CALTECH101; L - LABELME; S - SUN09; V - PASCAL VOC.

Table 18. Accuracy evaluated on VLCS; $d = 2$.

	Acc_{id}					Acc_{ood}				
	C	L	S	V	μ	C	L	S	V	μ
CENTRAL	-	-	-	-	-	-	-	-	-	-
LOCAL	57.1 ± 3.4	62.4 ± 5.0	64.2 ± 7.1	69.2 ± 5.3	63.2	63.4 ± 7.0	50.0 ± 3.0	44.2 ± 5.7	42.2 ± 4.7	50.0
FEDAVG	60.3 ± 1.8	65.4 ± 4.4	66.7 ± 6.4	70.0 ± 5.2	65.6	74.1 ± 1.0	56.0 ± 1.0	51.7 ± 0.4	49.1 ± 0.9	57.7
FEDPROX	59.3 ± 2.7	65.6 ± 5.2	65.4 ± 5.4	68.2 ± 4.6	64.6	73.4 ± 1.2	54.8 ± 0.5	50.7 ± 1.3	48.0 ± 1.8	56.7
PFEDHN	60.0 ± 3.2	63.5 ± 4.8	63.9 ± 6.8	68.5 ± 6.0	63.9	72.3 ± 2.9	54.6 ± 0.5	52.7 ± 2.1	48.5 ± 0.4	57.0
FEDSR	60.4 ± 2.9	66.3 ± 5.4	64.7 ± 6.3	69.4 ± 4.8	65.2	74.5 ± 1.0	53.2 ± 0.4	52.6 ± 0.7	49.6 ± 2.0	57.4
FEDGMA	61.2 ± 3.3	65.7 ± 3.5	66.8 ± 7.7	68.6 ± 5.7	65.6	72.1 ± 1.4	55.6 ± 0.6	51.4 ± 0.8	47.5 ± 0.6	56.7
hFEDF	61.2 ± 2.1	68.2 ± 4.6	66.9 ± 8.1	71.1 ± 5.3	66.8	74.8 ± 1.2	55.0 ± 1.5	53.1 ± 0.5	49.6 ± 1.0	58.1

ABBREVIATIONS: μ - AVERAGE; C - CALTECH101; L - LABELME; S - SUN09; V - PASCAL VOC.

Table 19. Accuracy evaluated on VLCS; $d = 3$.

	Acc_{id}					Acc_{ood}				
	C	L	S	V	μ	C	L	S	V	μ
CENTRAL	-	-	-	-	-	-	-	-	-	-
LOCAL	54.6 ± 3.2	59.4 ± 4.2	61.4 ± 2.8	60.0 ± 3.7	58.8	63.8 ± 6.1	51.3 ± 1.5	47.6 ± 2.1	43.8 ± 1.2	51.6
FEDAVG	61.1 ± 2.4	65.6 ± 3.8	66.5 ± 2.6	67.9 ± 2.7	65.3	72.8 ± 0.7	54.4 ± 0.4	53.7 ± 0.5	48.7 ± 1.1	57.4
FEDPROX	60.2 ± 2.9	64.6 ± 3.0	67.0 ± 1.6	68.9 ± 2.7	65.2	71.6 ± 0.6	53.5 ± 0.8	51.5 ± 0.5	48.0 ± 0.4	56.2
PFEDHN	59.6 ± 3.6	64.8 ± 3.4	65.6 ± 2.8	67.2 ± 3.0	64.3	71.6 ± 0.9	55.1 ± 0.7	51.8 ± 1.2	49.5 ± 1.0	57.0
FEDSR	60.6 ± 2.6	65.3 ± 2.9	67.8 ± 3.2	66.7 ± 2.7	65.1	71.7 ± 2.3	56.1 ± 0.7	53.5 ± 1.1	48.7 ± 1.0	57.5
FEDGMA	60.9 ± 3.6	65.3 ± 3.0	67.0 ± 2.5	68.2 ± 3.0	65.3	71.9 ± 0.7	55.3 ± 0.5	52.7 ± 0.2	48.7 ± 0.5	57.2
hFEDF	61.9 ± 2.9	66.7 ± 4.0	66.2 ± 2.2	68.1 ± 2.8	65.7	75.3 ± 1.5	55.7 ± 0.6	53.7 ± 1.5	50.1 ± 0.2	58.7

ABBREVIATIONS: μ - AVERAGE; C - CALTECH101; L - LABELME; S - SUN09; V - PASCAL VOC.

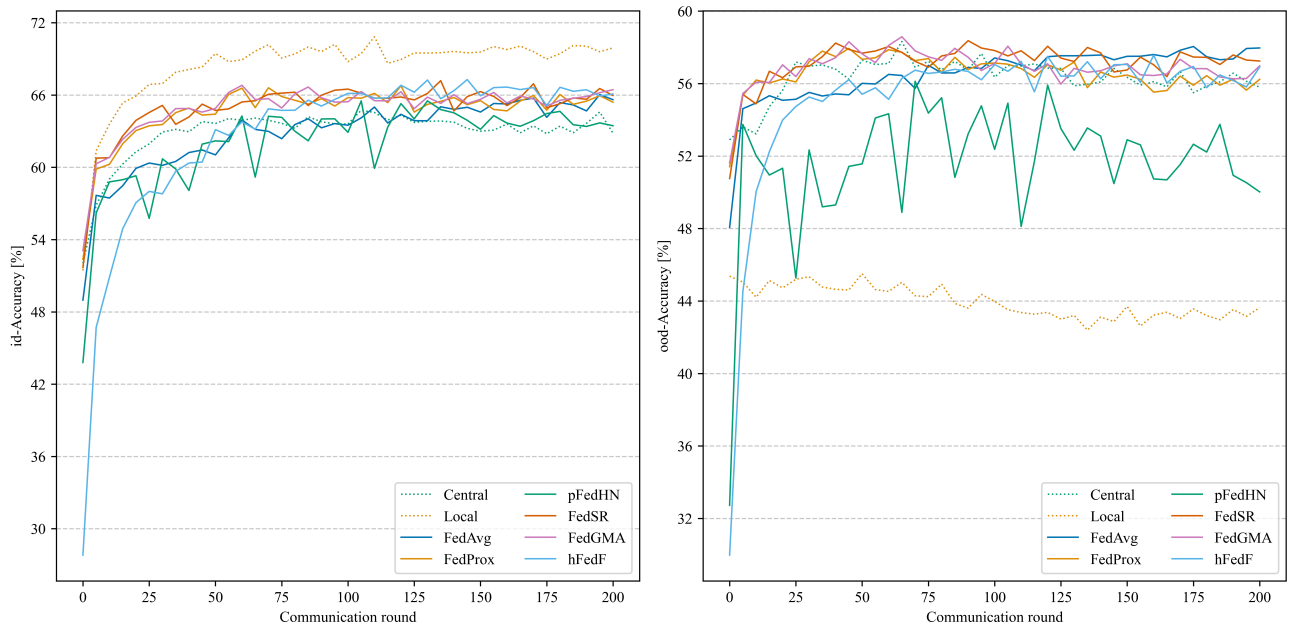


Figure 17. Evaluation curves. VLCS; $d = 1$.